Chronological and Morphological Study of Heart Development in the Rat

SALAZAR GARCÍA MARCELA,[1,2] REVILLA MONSALVE MARÍA CRISTINA,[3] PALOMINO GARIBAY MIGUEL ANGEL,[4] ARTEAGA MARTÍNEZ MANUEL,[5,6] DÍAZ-CINTRA SOFÍA,[7] DE LA ROSA-SANTANDER PATRICIA,[7] ROQUE-RAMÍREZ BLADIMIR,[8] AND SÁNCHEZ GÓMEZ CONCEPCIÓN[1]*

[1]Laboratorio de Investigación en Biología del Desarrollo y Teratogénesis Experimental, Hospital Infantil de México Federico Gómez
[2]Laboratorio de Citología, Escuela Nacional de Ciencias Biológicas, IPN
[3]Unidad de Investigación en Enfermedades Metabólicas, Centro Médico Nacional Siglo XXI. Instituto Mexicano del Seguro Social
[4]Colegio Ciencia y Tecnología, Universidad Autónoma de la Ciudad de México, UACM
[5]Facultad de Medicina, Universidad Nacional Autónoma de México
[6]Escuela de Medicina, Universidad Panamericana
[7]Departamento de Neurobiología del Desarrollo y Neurofisiología, Instituto de Neurobiología, Campus UNAM-Juriquilla
[8]División de Investigación Biomédica, Subdirección de Enseñanza e Investigación, CMN 20 de Noviembre, ISSSTE

ABSTRACT

Adult and embryonic laboratory rats have been used as a mammalian model organism in biomedical research, descriptive and experimental cardiac embryology, and experimental teratology. There have been, however, considerable variations and discrepancies concerning the developmental staging of the rat embryo in the reported literature, which have resulted in several controversies and inconsistencies. Therefore, we carried out a careful anatomical and histological study of rat cardiac morphogenesis from the premorphogenetic period to the mature heart in a newborn pup. A correlation between the chronology and morphological features of the heart and embryo or newborn was made. We provide a simple and comprehensive guide relating the developmental timing and fate of the embryonic components of the heart and their morphological changes in the rat based on *in vivo* labeling studies in the chick. We also compare the timing of heart development in rats, humans, and mice. Anat Rec, 295:1267–1290, 2012. © 2012 Wiley Periodicals, Inc.

Key words: heart development; cardiac embryology; rat embryonic development

INTRODUCTION

Cardiac development is a very complex and dynamic process, which ultimately results in the formation of a four-chambered heart from a single tubular structure. Although the definitive ventricles and atria represent discrete anatomical units, both are derived from diverse embryological components (primitive cardiac segments), which emerge at specific developmental stages during the torsion and looping process (de la Cruz and Markwald, 1998; de la Cruz et al., 2001). The *in vivo* labeling of chick embryos has significantly advanced our understanding of how the heart develops, including when the rudimentary

Grant sponsor: Hospital Infantil de México Federico Gómez; Grant number: HIM/2008/013.

*Correspondence to: Sánchez Gómez Concepción, PhD, Hospital Infantil de México Federico Gómez, Lab. de Investigación en Biología del Desarrollo y Teratogénesis Experimental. Dr. Márquez 162, Col. Doctores, Del. Cuauhtémoc. CP 06720, México, DF. E-mail: csgomez_2000@yahoo.com

Received 9 January 2012; Accepted 21 April 2012.

DOI 10.1002/ar.22508
Published online 19 June 2012 in Wiley Online Library (wileyonlinelibrary.com).

structures first appear, what their anatomic boundaries are, what morphological changes they undergo and how they contribute to the adult ventricles and atria (Castro-Quezada et al., 1972; de la Cruz et al., 1977; 1987; 1989; 1991; 1997; Anselmi and de la Cruz, 1998; Sánchez Gómez et al., 2005; Contreras Ramos et al., 2008). In addition, the rat is frequently used in descriptive and experimental cardiac embryology (Ya et al., 1998; Christoffels et al., 2000) and over the years it has proven to be an exponentially valuable animal model in experimental teratology and biomedical research (Christie, 1963; Rice and Barone, 2000; Simán et al., 2000, Daston et al., 2004; Marinho et al., 2007; Mashimo et al; 2008; Aitman et al., 2008; Twigger et al., 2008; Monti et al., 2008; Petretto et al., 2008; Geurts et al., 2009). Different studies, however, report considerable variation concerning the age at which a rat embryo reaches a specific developmental stage. The discrepancies are a result not only from strain differences but also from the methods used to stage embryos and to estimate the time of mating as presence of a vaginal plug and/or spermatozoa in the vaginal smear. In addition, there is a lack of detailed information on the external morphological features of the newborn rat, and there is even less information of the heart. Based on these facts, the aim of this article was to prepare a series of heart stages in the developing and newborn rat that correlate with the morphological changes taking place in the organism, the morphological features of the heart, and the chronological age. To establish the age at which each primitive cardiac segment appears, we carried out a careful anatomic and histological study of cardiac development in the rat from the premorphogenetic period (cardiogenic areas) to the emergence of the four-chambered heart (mature heart). The newborn heart was also analyzed. Descriptions were primarily based on the *in vivo* labeling findings of the chick embryo heart. We also compared the timing of heart development in rats, humans, and mice.

MATERIALS AND METHODS

Sprague Dawley rats were mated to collect at least 30 embryos at each of the following embryonic days (ED): 9 (at 8:00 AM on Day 9 after mating), 9 + 10 hr (at 6:00 PM on Day 9 after mating), 9 + 15 hr (at 11:00 PM on Day 9 after mating) and 10–16 (at 8:00 AM in all cases). The same number of fetuses (17–20 days) and newborn pups (21 days) were also obtained. The morning on which spermatozoa were found in the vaginal smear was considered to be ED 0. To harvest embryos, pregnant females were anesthetized with diethyl ether inhalation, immediately afterwards perfused with 3.5% formaldehyde in phosphate buffered solution (PBS) and hysterectomized. After overnight fixation, each conceptus was removed from the uterus, and extraembryonic membranes were excised to acquire the embryos. Newborn pups were obtained during parturition immediately after they were born. Fetuses and newborn organisms were sacrificed by diethyl ether inhalation and fixed in 3.5% formaldehyde for 48 hr. They were weighed, and the crown to tail length was recorded. Some pregnant animals were hysterectomized after diethyl ether inhalation to collect embryos to perform histological analysis and whole-mount *in situ* hybridization. In all cases, animal procedures were approved and performed in accordance with institutional guidelines (NOM-062-ZOO-1999).

Anatomic Studies

To make the cardiogenic fields in evidence, ruthenium red staining of the extracellular matrix (Linash and Lash, 1987) and *Nkx 2.5* whole-mount *in situ* hybridization were performed in embryos at Day 9 + 10 hr. In the first case, the fixed embryos still enclosed within the extraembryonic membranes, were immersed in 3.5% formaldehyde and 0.5% ruthenium red solution for 72 hr. The specimens were then immersed in 0.3 N magnesium chloride for 48 hr and rinsed in PBS. In the second case, digoxigenin-labeled Nkx2.5 antisense mRNA probes generated by *in vitro* transcription according to standard protocols generously provided by Dr. Ramón M Coral-Vázquez (Subdirección de Enseñanza e Investigación, CMN "20 de Noviembre" ISSSTE, México, DF) were used. The specimens previously collect in PBS with fetal calf serum (5%) were fixed overnight in freshly prepared 4% paraformaldehyde. They were dehydrated in a graded methanol series in PBT (PBS with 0.1% Tween-20) and stored in absolute methanol at −22°C. The specimens once rehydrated, were treated with 35 μg/mL proteinase K dissolved in PBST for 10 min at 21°C. Hybridization with the Nkx2.5 antisense mRNA probes was performed at 65°C. Probe binding to the cardiogenic fields was immunologically detected using sheep antidigoxigenin Fab fragment covalently coupled to alkaline phosphatase and NBT/BCIP as chromogenic substrate according to the manufacturer's protocol (Roche).

To determine the external and internal anatomic features of the heart from ED 12 to newborn pups, the intact or dissected hearts were photographed using an Olympus stereomicroscope SZH equipped with either a Nikon Coolpix 4500 digital camera or a Carl Zeiss stereomicroscope Lumar V12 and an Axiocam MRC. As a complement, at least three whole or dissected embryos and hearts of each age group (ED 9 + 15 hr to ED 16) were used for SEM analysis. In this case, the samples were dehydrated using a graded ethanol series, desiccated under liquid CO_2 with a critical-point drying apparatus (Samdri, 789A) and gold sputter coated (35 nm) in a Denton Vacuum Desk 1A apparatus. Photographs were taken using a SEM JEOL JSM 5300 at 15 kV.

Histological Analysis

Nine specimens from each group were fixed with alcoholic Bouin's solution for 24 hr and then rinsed in 70% ethanol. Immediately thereafter, they were dehydrated in a graded ethanol series, treated with cedar oil and embedded in paraplast (Oxford Labware). Frontal and sagittal 5-μm serial sections were stained with hematoxylin and eosin or alcian blue and azocarmine. Photographs were taken using an Olympus BH-2 RFCA optical microscope and a Nikon Coolpix 4500 digital camera.

RESULTS AND DISCUSSION

Premorphogenetic Period

ED 9 embryos. Cardiogenic areas. Tree-layered embryos with the fully elongated primitive streak

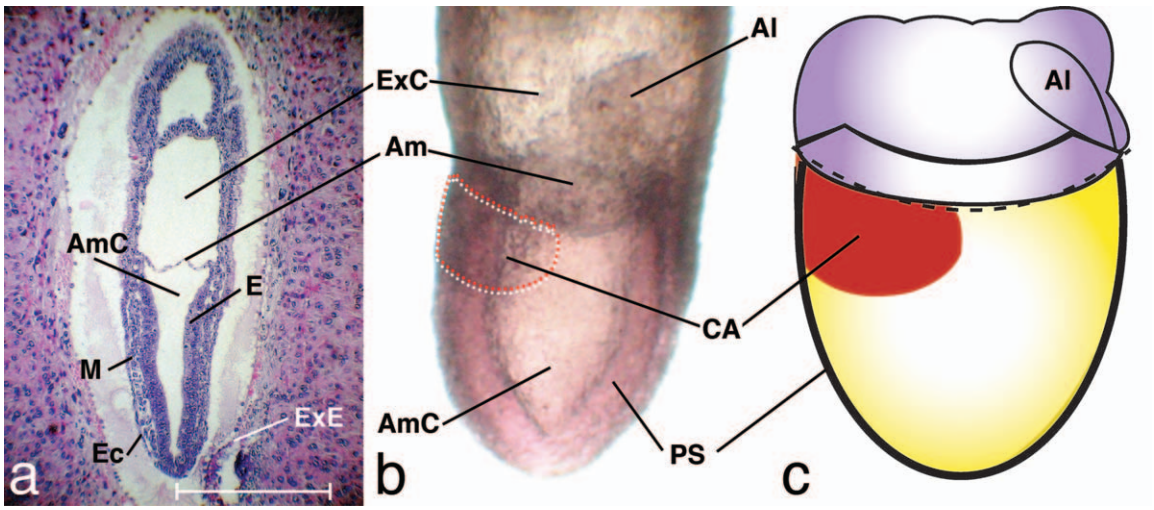

Fig. 1. ED 9 embryo. Pre-morphogenetic period of the heart I. **a, b, c**. Histological section, sagittal view, and schematic representation of the embryo displaying a tree-layered, presomitic cup containing cardiogenic areas (CA). Al, allantois; Am, amnion; AmC, amniotic cavity; E, endoderm; Ec, ectoderm; ExC, exocoelomic cavity; M, mesoderm; PS, primitive streak. Scale bar 0.4 mm.

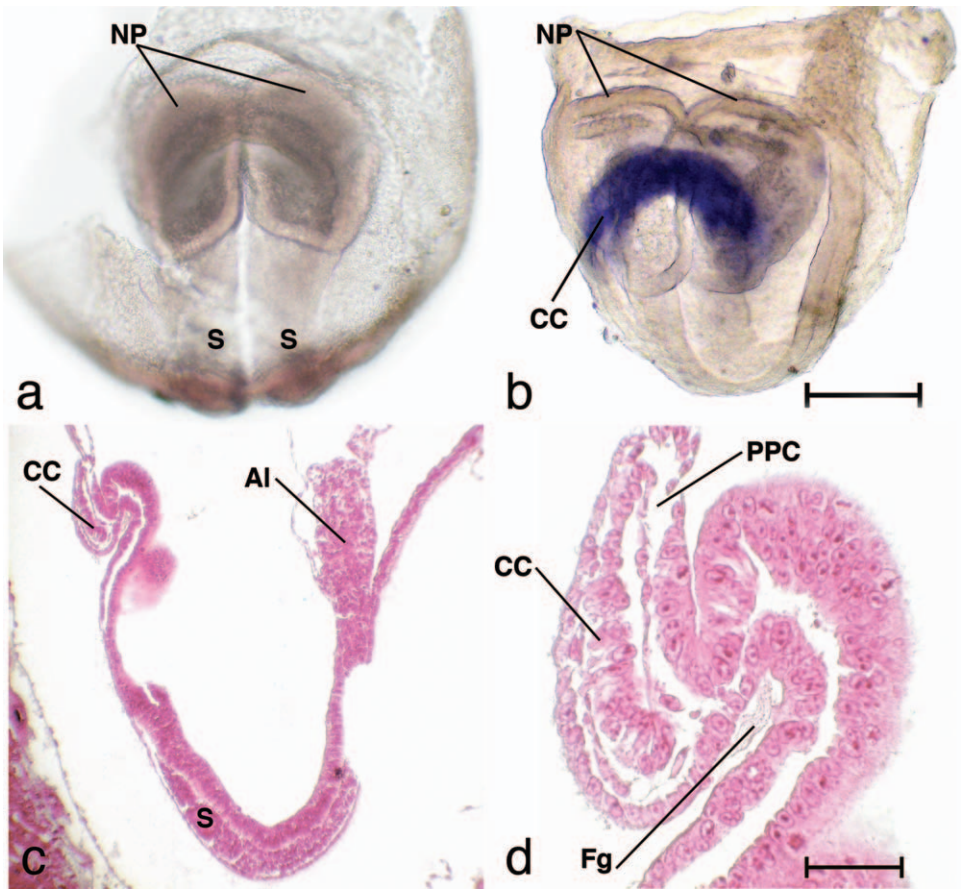

Fig. 2. Embryo at 9 days + 10 hr. Pre-morphogenetic period of the heart II. Frontal views of embryos stained with ruthenium red (**a**) and a whole-mount *in situ* hybridization showing *Nkx2.5* expression (**b**). Observe the cephalic neural plate (NP) and the cardiac crescent (CC). Scale bar 0.3 mm. **c, d**. Histological sagittal sections of the embryo. **c**. Notice the U-shaped embryonic body, the allantois (Al) and some somites (S). **d**. Observe the incipient foregut (Fg), the cellular organization of the cardiac crescent (CC) and the primitive pericardial cavity (PPC). Scale bar 0.05 mm.

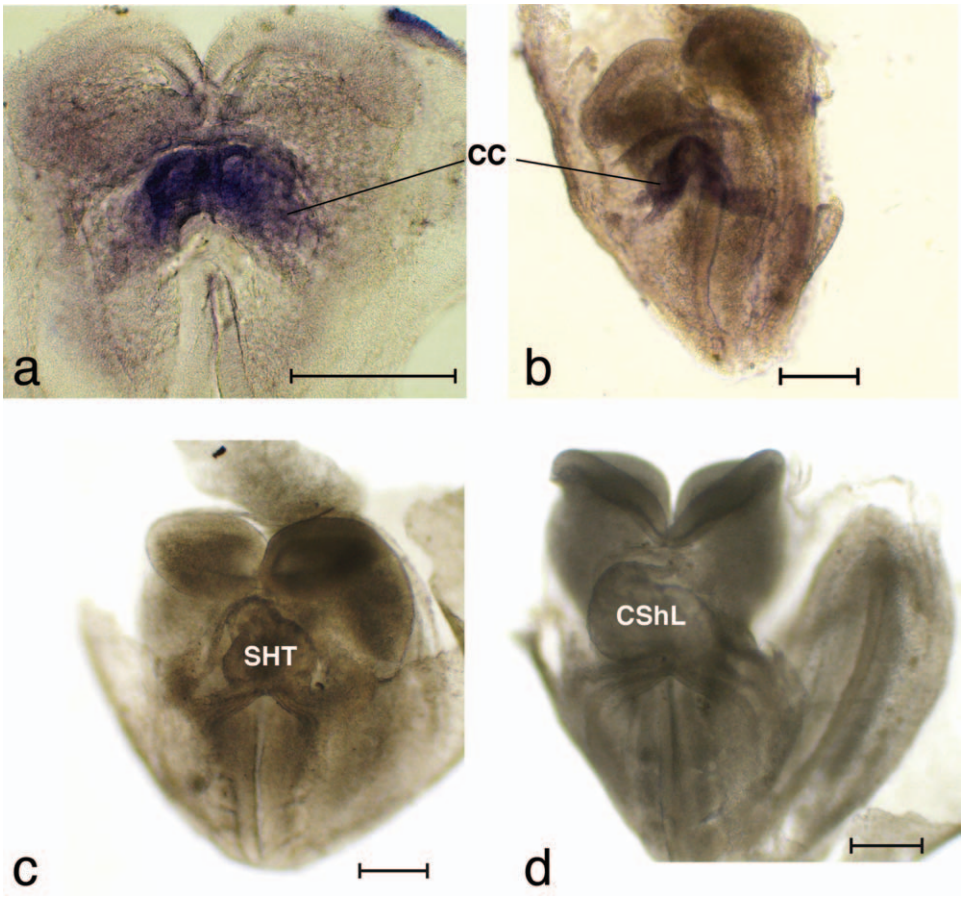

Fig. 3. Transition from the cardiac crescent period to the beginning of the torsion and looping process. **a, b**. Whole-mount *in situ* hybridization showing *Nkx2.5* expression within the entire cardiac crescent of embryos at ED 9 + 10 hr. **c, d**. Embryos at ED 9 + 15 hr with the embryonic body less curved than at earlier stages. Notice the "Straight heart tube" (SHT) and the "C-shaped looped heart" (CShL). Scale bars a =0.35 mm; b, c, d = 0.27 mm.

growing from its most posterior end to the anterior midline were observed (Fig. 1a,b). The primitive endoderm was seen outside of the amniotic cavity and covered by extraembryonic endoderm (Fig. 1a). Morphological expression of the heart is not yet visible. Based on the results from fate mapping studies in the mouse (Parameswaran and Tam, 1995; Tam et al., 1997; Tam and Schoenwolf, 1999), however, we can infer that the precardiac mesoderm at this stage has formed two elliptical bilateral areas that grow from the level of Hensen's node and extend caudally a quarter of the distance of the primitive streak (Fig. 1b,c). A comparable developmental stage has been described in stage 10 mouse embryos at 7 days post coitum (dpc), (Theiler, 1989; Kaufman, 1999; Tam and Schoenwolf, 1999), stage 4HH chick embryos (Rawles, 1943; Hamburger and Hamilton, 1951; Redkar et al., 2001), and Carnegie Stage VI–VII human embryos (O'Rahilly and Muller, 1987).

ED 9 + 10 hr embryos. Cardiac crescent. As previously described, the U-shaped embryonic body at this age displayed a dorsal concavity (Fig. 2c) and the surface of the neural ectoderm fold was visible. The incipient neural fold extended the entire length of the embryonic body and had a wide, shallow cranial region, which corresponded to the neural plate (Fig. 2a,b). In addition, five pairs of somites were also identified. In the sagittal view the incipient anterior intestinal portal or foregut appeared as an inverted U-shaped, wide, rostro-ventral sulcus (Fig. 2c,d). The ruthenium red staining and Nkx2.5 mRNA expression at ED 9 + 10 hr embryos showed the horseshoe-shaped cardiac crescent on the ventral side of the embryo beneath the foregut (Fig. 2a,b). This result coincides with findings in mice by Lints et al., (1993) and Heikinheimo et al. (1994). Histological analysis revealed the primitive pericardial cavity and polyhedral pre-myocardial cells intermingled with a plexus of endothelial strands (Fig. 2d). A similar cardiac crescent has been described in stage 11 mouse embryos at 7.5 dpc (Theiler, 1989; Parmacek and Leiden, 1999), stage 7HH chick embryos (Stalsberg and deHaan, 1969; Redkar et al., 2001), and one somite Carnegie Stage IX human embryos (Davis, 1927).

Morphogenetic Period

The transition from the cardiac crescent (ED 9 + 10 hr) to the beginning of the morphogenetic period of heart development (ED 9 + 15 hr) was accompanied by changes in both the heart forming region features an the body

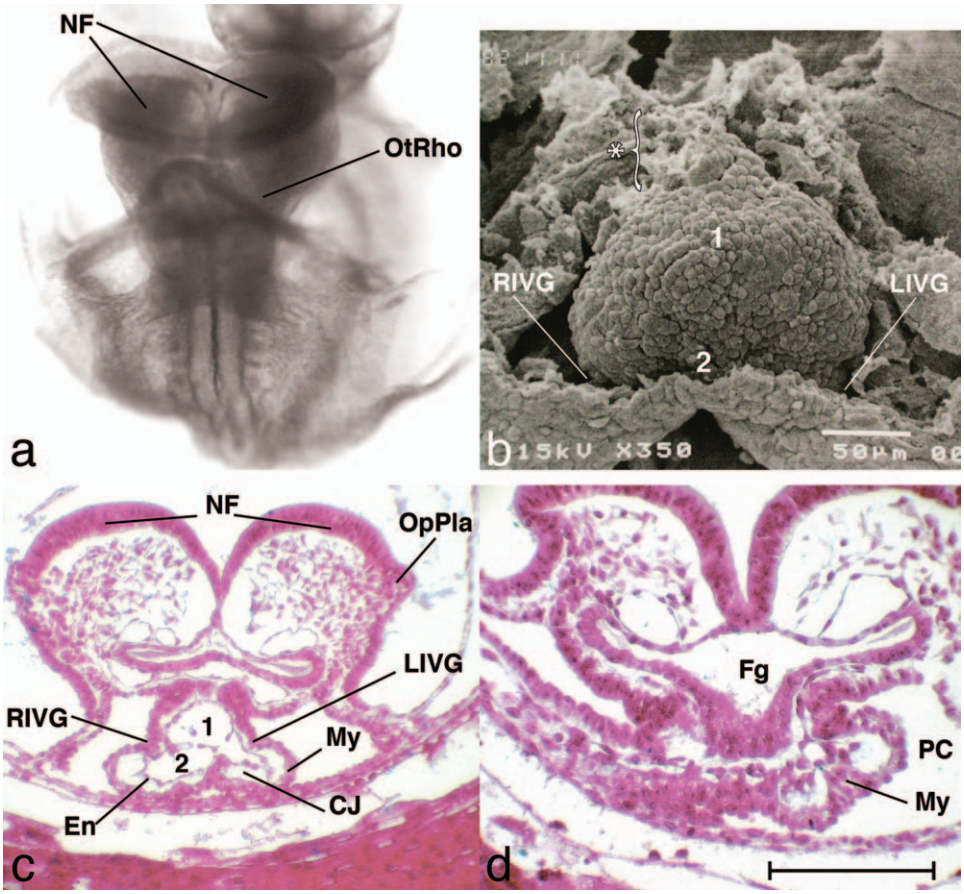

Fig. 4. Embryo at 9 days + 15 hr. Straight heart tube. **a, b**. Frontal views of the embryo. **a**. Observe the dorsally elevated neural folds (NF) and the otic rhombomere (OtRho). b. Scanning electron micrograph shows the "straight heart tube" formed by two primordia delimited by the right (RIVG) and left (LIVG) interventricular grooves. The asterisk highlighted a no well organized cell population, emerging from the pharyngeal mesoderm anterior to the heart **c**. Frontal section of the embryo. Observe the histological constitution of the heart and the optic placoda (OpPla). **d**. Transversal histological section of the embryo showing the incomplete dorsal wall of the heart. 1 = primordium of the apical trabeculated region of the right ventricle; 2 = primordium of the apical trabeculated region of the left ventricle. CJ = cardiac jelly; En = endocardium, Fg = foregut; My = myocardium. Scale bar = 0.1 mm.

morphology. At each age, the embryo was curved to a lower extent because the dorsal concavity of the U-shaped embryonic body gradually becomes less deep (Fig. 3).

ED 9 + 15 hr embryos. In accordance with the study by Kaufman (1999) in 8.0 dpc mouse embryos, we observed two different embryonic and cardiac morphologies within the same litter (Figs. 4, 5).

1. **Straight heart tube.** The heart was bilaterally symmetric displaying a broad cephalic and a smaller caudal segment. Between both segments there were two shallow grooves (Fig. 4b,c). Interestingly, a not well-organized cell population, emerging from the pharyngeal mesoderm was observed anterior to the early heart tube (Fig. 4b). We suppose that these cells highlighted by an asterisk in Fig. 4b correspond to the anterior heart field that had begun to specify almost at the same time that the straight heart tube was forming. These facts indicate that in the rat transformation of the anterior heart field into cardiac structures takes place earlier and faster than in the chick. Moreover, straight heart tube to C-shaped looped heart transition takes around 15 hr in the chick embryo. In contrast, we could almost always recognize this progressive morphological transformation of the heart in embryos of the same litter at ED 9 + 15 hr. We think this could be the reason for the difference because it has been reported that in mice the myocardium of the left ventricle and the atria come from the primary heart-forming field, while myocardium of the right ventricle and the embryonic outflow are delivered from the anterior or secondary heart-forming field (Zaffran et al., 2004). Therefore, based on our observations in rat, findings in mice (Zaffran et al., 2004) and previous *in vivo* labeling studies in the chick embryo (de la Cruz et al., 1989; de la Cruz and Sánchez Gómez, 1998), we infer that the anterior zone of the broad cephalic region of the straight heart tube in the rat will contribute to the development of the apical trabeculated region of the right ventricle, while the rest of the cardiac tube at this age, except the incipient caudal segment, will form the apical trabeculated region of the left ventricle. The cells that we observed in the pharyngeal

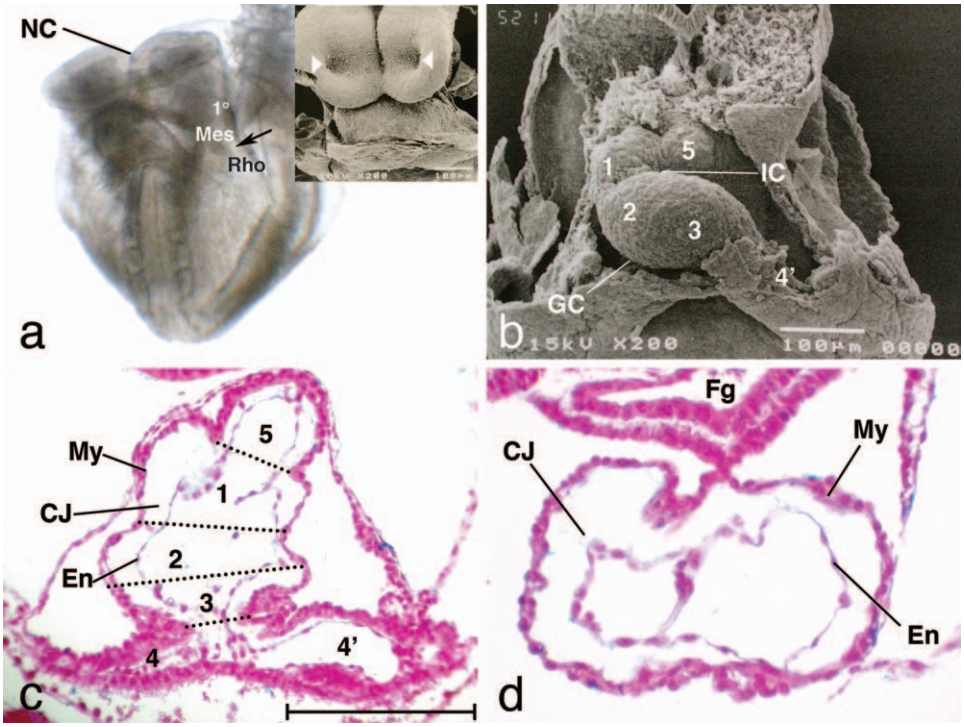

Fig. 5. Embryo at 9 days + 15 hr. C-shaped looped heart. **a, b**. Frontal views of the embryo. **a**. Observe the cephalic incipient neural canal (NC) and the superficial boundary (arrow) between the mesencephalon (Mes) and rhombencephalon (Rho). **Inset** shows the well-defined optic pit foveae (arrowheads). **b**. Scanning electron micrograph of a C-shaped looped heart, notice five distinctive primordia. **c**. Histological frontal section of the heart depicting the cardiac wall displaying myocardium (My), endocardium (En) and cardiac jelly (CJ). **d**. Transversal section of the heart showing the myo-endocardial wall of the heart tube. 1, 2 = primordium of the apical trabeculated region of the right ventricle and of the left ventricle, respectively; 3 = primitive inlet (atrioventricular region); 4, 4′ = right and left primitive atria, respectively; 5 = proximal segment of the embryonic outflow tract (conus); Fg = Foregut; IC = inner curvature; GC = greater curvature. Scale bars = 0.25 mm.

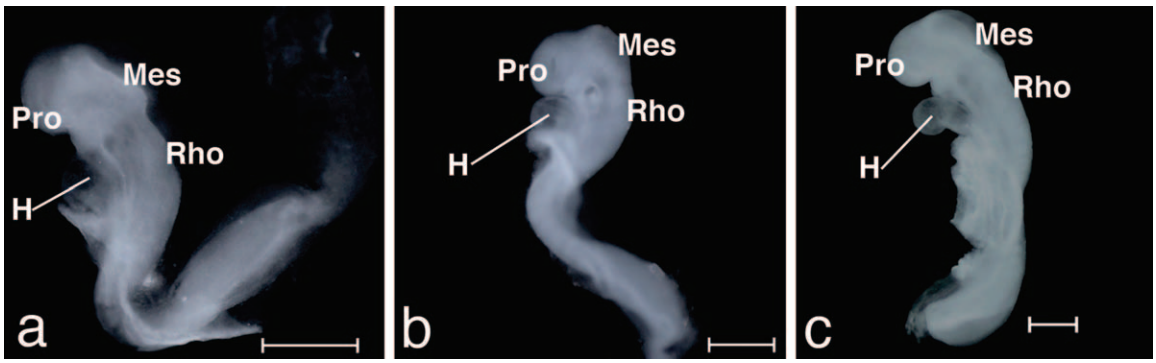

Fig. 6. Changes in the external features of the embryo between ED 9.5 and 10. Notice that the embryonic body becomes quite straight. H = heart; Mes = mesencephalon; Pro = prosencephalon; Rho = rhombencephalon. Scale bars = 0.5 mm

mesoderm, anterior to the early heart tube (Fig. 4b) must be involved in formation of the conus.

2. **C-shaped looped heart** (Fig. 5). As in the chick embryo at stage 12HH (de la Cruz, 1998a; Mannër, 2000), the previously open cardiac trough had been transformed into a bilaterally asymmetric myo-endocardial tube, not yet covered by the epicardium (Fig. 5b–d). Histological analysis and azocarmine staining showed the recently fused dorsal borders of the myo-endocardial mantle (Fig. 5d) and abundant cardiac jelly or acellular ECM between the myocardium and endocardium (Fig. 5c,d). This heart has been designated a "C-shaped looped heart" because, in a frontal view, its convex border (greater curvature)

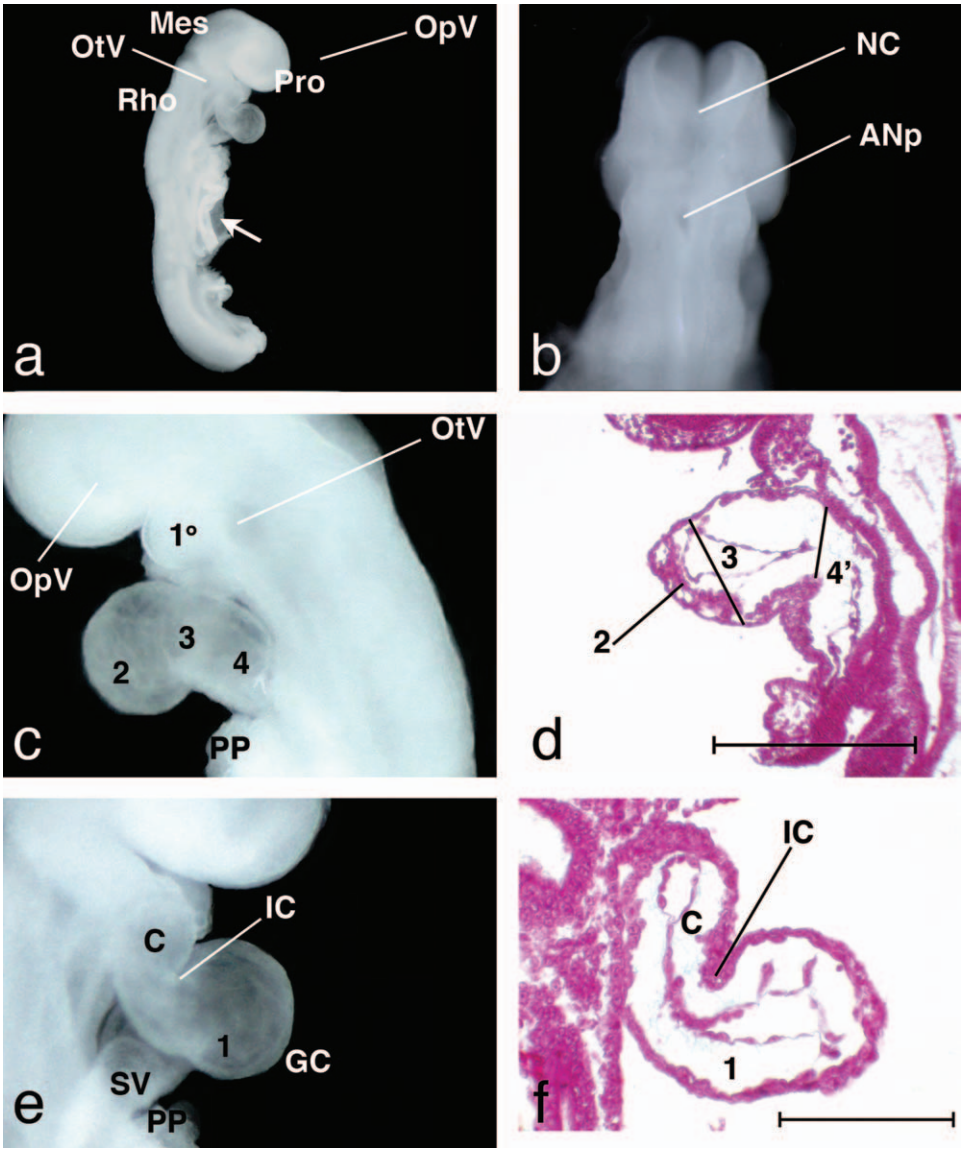

Fig. 7. Embryo at 10 days. Ventrally convex and dorsally concave immature S-shaped heart loop. **a**. The right view of a whole embryo shows three primary brain vesicles, the small otic vesicle (OtV) and the optic vesicle (OpV). Observe the opening between the intra- and extraembryonic coelom (arrow). **b**. Dorsal view of the cephalic region of the embryo. Observe the dorsally elevated neural folds (NF) and the zone of the future anterior neuropore (ANp). **c, d**. A left view and sagittal histological section depicting the well-developed first pharyngeal arch (1°), the left primitive atria (4′), the embryonic inlet (3) and the primordium of the apical trabeculated region of the left ventricle (2). **e, f**. Right view and sagittal histological section of the heart. Observe the primordium of the apical trabeculated region of the right ventricle (1) and the proximal segment of the embryonic outflow (C). PP = proepicardial protrusion; SV = sinus venosus. IC = inner curvature; GC = greater curvature. Other abbreviations are as in previous figures. Scale bars = 0.25 mm.

can be seen to the right, while its concave surface (inner curvature) is observed to the left (Fig. 5b). Based on experimental *in vivo* labeling results in the chick embryo, we infer that in rat the C-shaped looped heart is composed of five primordia (Fig. 5b) organized in a caudo-cranial sequence as follow: I. The caudal region of the C-looped heart corresponds to the right and left primitive atria (Castro Quezada et al., 1972). This structure circumscribes the anterior intestinal portal and has a myo-endocardial crescent shape which is separated from the C loop by a shallow right and a deep left atrioventricular (AV) grooves. II. The middle region (C loop) has two limbs delimited by a deep groove called inner curvature or left interventricular groove (Fig. 5b). By *in vivo* labeling in the chick embryonic heart, we know that the caudal limb displays two primordia: the primitive inlet (AV region) and the primordium of the apical trabeculated region of the left ventricle (de la Cruz et al., 1987; 1991). The cephalic limb of the cardiac loop corresponds to the primordium of the apical trabeculated region of the right ventricle (de la Cruz et al., 1989). III. The most cephalic region of the heart represents the caudal zone of the conus (de la Cruz et al., 1977) which has recently been

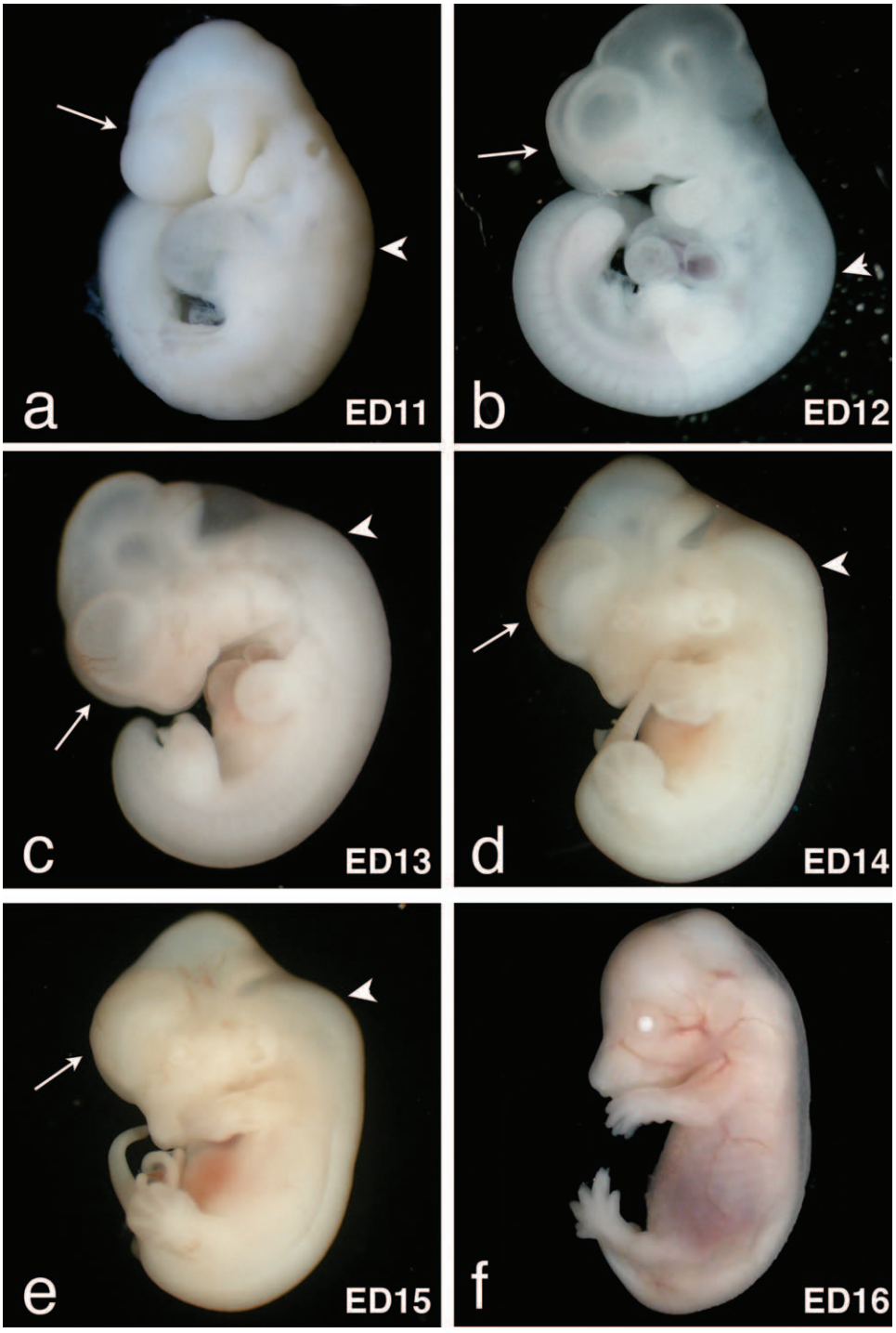

Fig. 8. Changes in the external feature of the embryonic body. Left views of ED 11-16 embryos showing that the cranial (arrow) and cervical (arrowhead) flexures determine the external feature of the embryonic body. Labels of the anatomical structures are shown in subsequent figures.

designated the proximal segment of the embryonic outflow tract (Anderson et al., 2003, Sánchez Gómez et al., 2005). It is essentially a vertically-oriented right myo-endocardial tube with a caudal border represented by the cono-ventricular grooves while its rostral end leads to the first aortic arches.

ED 10 embryos. Ventrally convex and dorsally concave immature S-shaped heart loop. It is interesting to note that between ED 9.5 and 10 the most dorsal edge of the neural folds gradually roll inward to form the neural tube. At the same time, the external features of the embryonic body were slowly modified

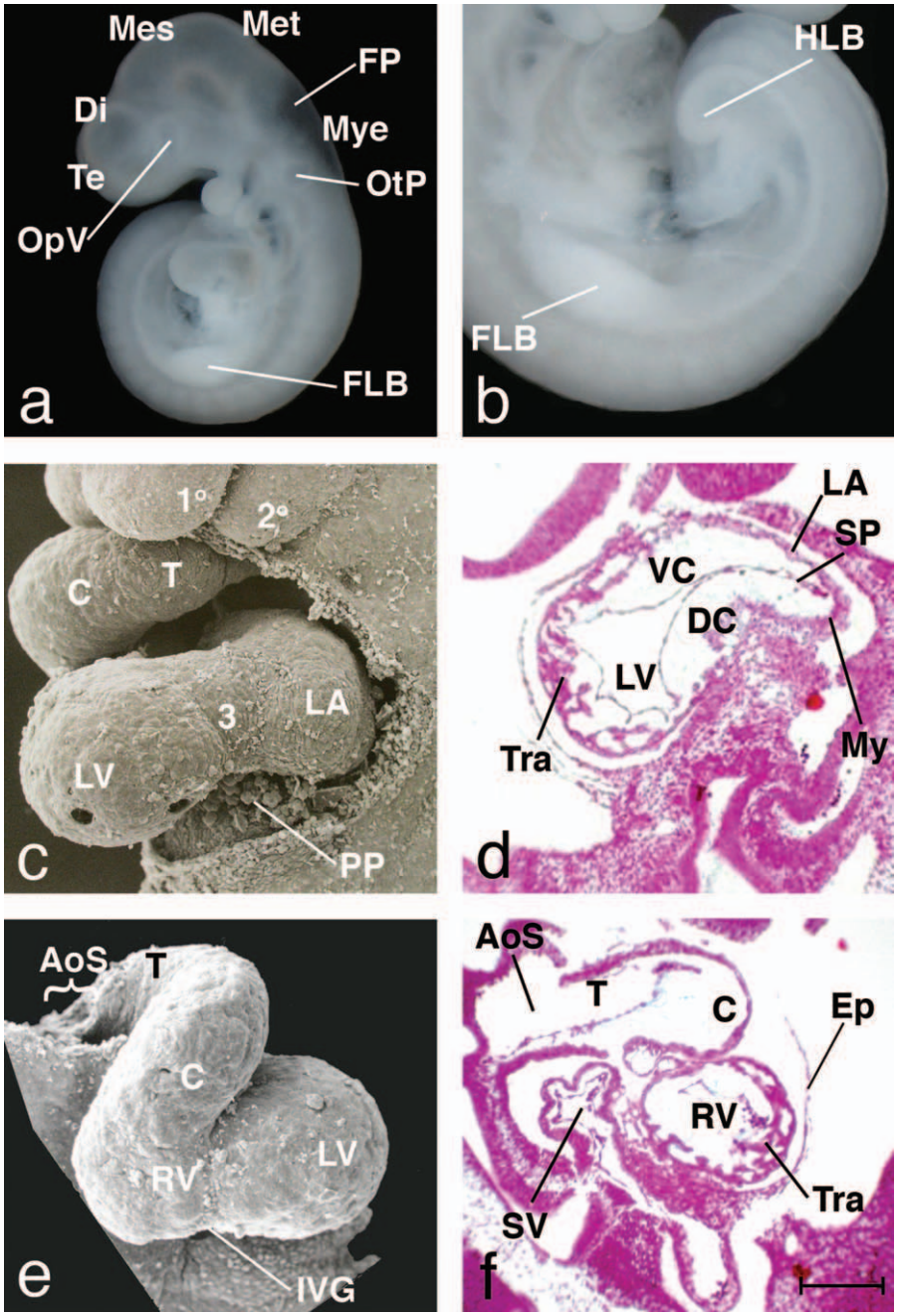

Fig. 9. Embryo at 11 days. Beginning of cardiac septation. **a**. Left view of a whole embryo depicting the smoothly delineated secondary brain vesicles, telencephalon (Te), diencephalon (Di), mesencephalon (Mes), metencephalon (Met) and myelencephalon (Mye). The optic vesicles (OpV), otic pits (OtP) and forelimb bud (FLB) are also showed. **b**. Right view of the caudal region of the embryo. Observe the incipient hindlimb bud (HLB). **c, d**. Left view and sagittal histological section of the heart. Notice the well developed proepicardial protrusion (PP) and the cardiac cavities externally coved by the primitive epicardium (Ep). The incipient dorsal (DC) and ventral (VC) cushions inside the embryonic inlet (3) and the developing left ventricle (LV) with small individual trabeculations (Tra) are also depicted. **e, f**. Right view and sagittal histological section of the heart. Observe the Aortic Sac = AoS, the proximal (C) and distal (T) segments of the embryonic outflow tract and the small individual trabeculations (Tra) inside the developing right ventricle (RV). SP = Septum primum 1°, 2° = pharyngeal arches. Other abbreviations have been listed in previous figures. Scale bars = 0.25 mm.

(Fig. 6). These events resulted in some ED 10 embryos that were almost straight and had 16–18 pairs of somites. The neural canal of these embryos extended cranially to the border of the first somite and caudally beyond the last one (Fig. 7a). The rostral boundary of the neural tube was frequently found open (Fig. 7b), and the caudal neuropore was open in all embryos at this stage. This finding indicates that there is no exact

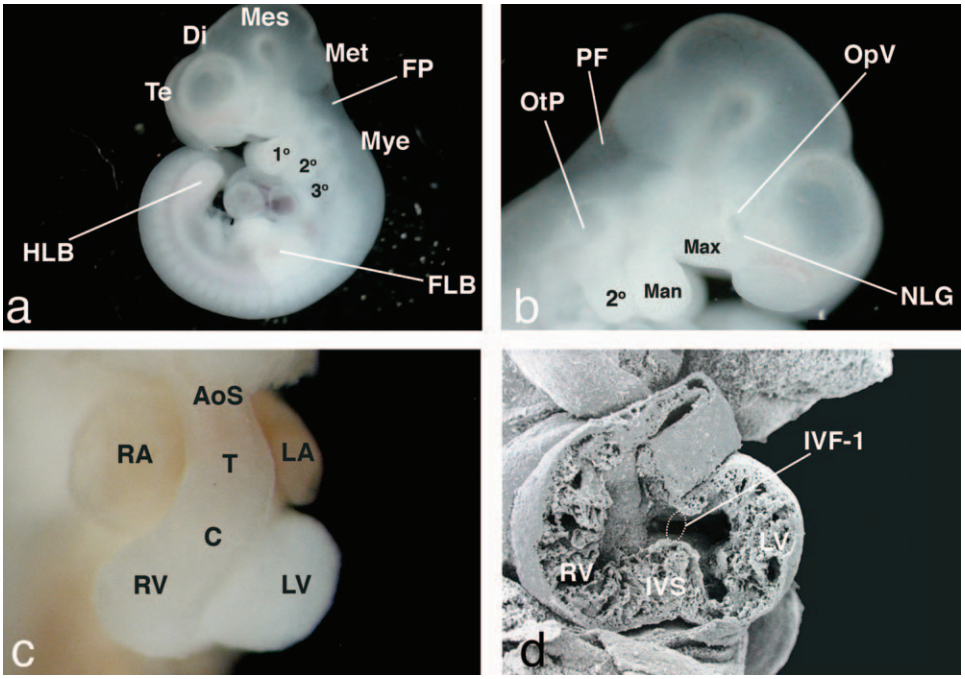

Fig. 10. Embryo at 12 days. **a**. Left view of a whole embryo showing the secondary brain vesicles, two well developed (1°, 2°) and one emerging (3°) pharyngeal arches. Notice the shallow pontine flexure (PF), the fin-shaped hindlimb (HLB) and forelimb bud (FLB). **b**. Right view of the cephalic region of the embryo depicting the otic pit (OtP), the optic vesicle (OpV), the incipient naso-lacrimal groove (NLG), the mandible (Man) and the maxillary (Max) components of the first pharyngeal arches. **c, d**. Frontal view and scanning electron micrograph of the heart showing the cephalo-dorsally positioned atria. IVF-1 = primary interventricular foramen; IVS = interventricular septum. Other abbreviations have been listed in previous figures.

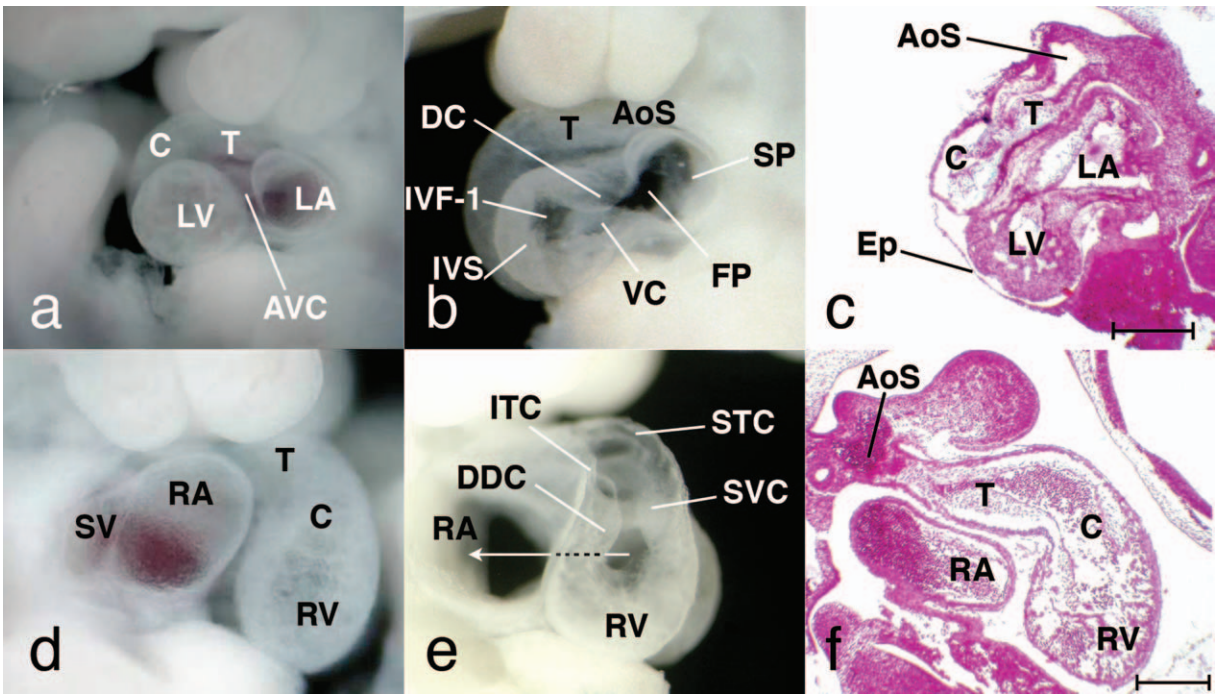

Fig. 11. Heart of an embryo at 12 days. Projection of the aortic sac into the pericardial cavity. **a, b, c**. Left views of the heart. Observe the developing left atrium (LA) and the left ventricle (LV) connected by the atrioventricular canal (AVC). **b**. Notice the "primitive cardiac septum" comprised of the septum primum (SP), the dorsal (DC) and ventral (VC) atrioventricular cushions and the developing interventricular septum (IVS). The foramen primum (FP) and the primary interventricular foramen (IVF-1) are also observed. **c**. Histological features of the anatomic components of the primitive cardiac septum. **d, e, f**. Right views of the heart show the proximal (C) and distal (T) segments of the embryonic outflow tract emerging from the right ventricle (RV), which is connected to the right atrium (RA) by the atrioventricular canal (arrow). DDC = dextrodorsal conus crest; SV = sinus venosus; SVC = sinistroventral conus crest; STC = superior truncus crest; ITC = inferior truncus crest. Other abbreviations are as in previous figures. Scale bars = 0.3 mm.

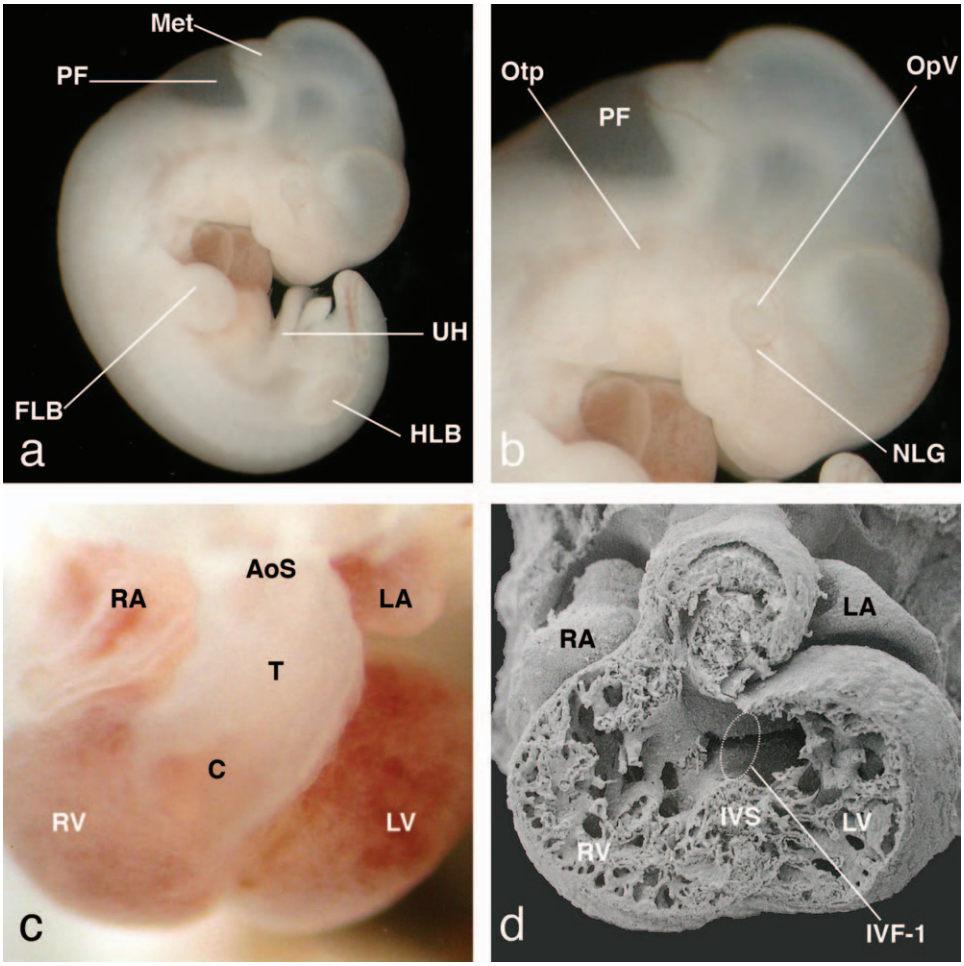

Fig. 12. Embryo at 13 days. **a, b**. Left views of the embryo. **a**. Notice the well-developed pontine flexure (PF), the reduced metencephalon (Met), the paddle-shaped forelimb (FLB) and the fin-shaped hindlimb (HLB) bud. **b**. Observe the relatively long naso-lacrimal groove (NLG) and the oval otic vesicle (OtV). **c, d**. Frontal view and scanning electron micrograph of the heart. **d**. Notice the incompletely developed interventricular septum (IVS) and the primary interventricular foramen (IVF-1). UH = physiological umbilical hernia. Other abbreviations have been listed in previous figures.

equivalent for the rostral neuropore in the rat as described in humans (Streeter, 1942). The three primary brain vesicles, prosencephalon (forebrain), mesencephalon (midbrain) and rhombencephalon (hindbrain) were well defined (Fig. 7a). Furthermore, the first pharyngeal pouch was in contact with the ectoderm (Fig. 7a,c), and in some embryos the second pharyngeal arch had begun to evaginate. The otic vesicles were not easily recognized, but the optic vesicles could easily be identified (Fig. 7a). The lateral body folds were more elevated at this age (Compare Figs. 6, 7a), but a wide opening remained between the intra- and extraembryonic coelom (Fig. 7a). The forelimb buds appeared as two small elevations on the lateral surface of the embryonic wall at the 6–9 somite level. The rat embryo morphology was similar to that of the stage 14 mouse embryos at 8.5–9 dpc with 13–22 pairs of somites (Theiler, 1989, Kaufman, 1999) and the Carnegie Stage XI–XII human embryos containing 13–14 somites.

The S-shaped heart loop was ventrally convex and dorsally concave and the dorsal mesocardium has disappeared. This cardiac shape recently has been referred to as an "immature S-loop" by Mannër (2009). Moreover, we found as was described in the chick embryos heart at stage 14-15HH (Mannër and Merkel; 2007), that the bilaterally symmetric right and left sinus horns connected to the primitive atria, which were partially displaced to the cephalic region and had begun to acquire a dorsal position (Fig. 7c,d). Both the sinus horns and primitive atria were formed by compact myocardium covered by endocardium (Fig. 7d). The atria and the ventrally positioned ventricular region (greater curvature) remained connected by the common embryonic inlet (Fig. 7c,e). Some spaces were observed between myocytes in the ventricular myocardial sleeve (Fig. 7d,f). The inner curvature or concave surface of the heart loop had a dorso-superior position (Fig. 7e,f). The proximal tubular segment of the common embryonic outflow tract (conus) has grown mainly in length and was still found to be in a cephalic position. It was directed dorso-ventrally and connected to the cephalic limb of the loop (Fig. 7e,f), which corresponds to the primordium of the trabeculated region of the right ventricle (de la Cruz et al., 1977, 1989). At this stage, the distal segment of

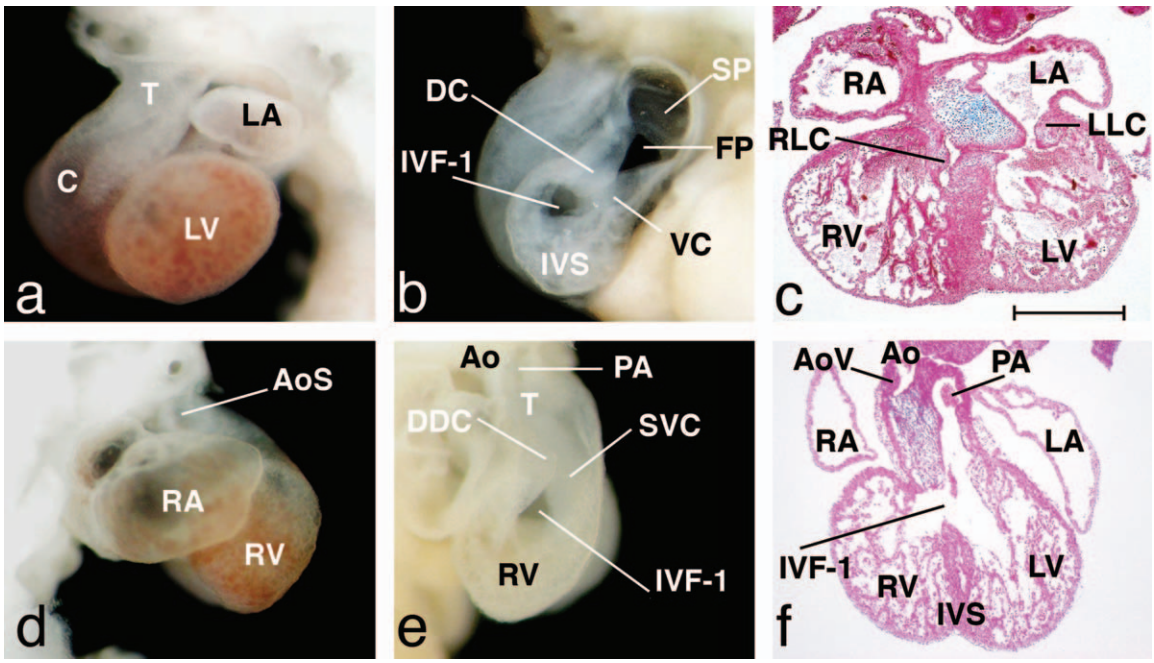

Fig. 13. Heart of the embryo at 13 days. End of the torsion and looping process and division of aortic sac into two ducts. **a, b**. External view and dissection of the left cavities of the heart. **b**. Observe the "primitive cardiac septum" composed of the septum primum (SP), the overlapping dorsal (DC) and ventral (VC) atrioventricular cushions and the partially developed interventricular septum (IVS). The Foramen primum (FP) and the primary interventricular foramen (IVF-1) are also shown **c**. A frontal histological section of the heart depicting the emerging right (RLC) and left (LLC) lateral cushions of the atrioventricular canal. **d, e**. Right views of the heart. **e**. Observe the voluminous dextrodorsal (DDC) and sinistroventral (SVC) conus crest. **f**. A frontal histological section of the heart shows the developing aortic valves (AoV) and the connection between the aorta (Ao) and the left ventricle (LV). PA = Pulmonary artery. Abbreviations are as in previous figures. Scale bars =0.35 mm.

the embryonic outflow tract (classically designated as the truncus arteriosus) could not yet be identified. Both the myocardium and endocardium of the primitive inlet (AV region) and the proximal segment of the embryonic outflow tract were separated by an abundant amount of acellular ECM or cardiac jelly (Fig. 7d,f). Despite having proepicardial protrusions on the ventral wall of the sinus horns (Fig. 7c–e), the heart was not yet covered by the epicardium (Fig. 7d,f). Nearly all of the references describe similar heart morphology in the 9.0 dpc mouse embryo, except Moorman et al. (2003), who categorized this stage as 9.5 dpc.

ED 11 embryos. Beginning of cardiac septation. From this age to 16 dpc, the cranial and cervical flexures cause a gradual change in the external feature of the embryonic body (Fig. 8). At 11 dpc, the embryo body has now turned over with the tail folded in and contains about 24 pairs of somites (Figs. 8a, 9a). The average crown to rump length of the embryos was 2.5 mm. The secondary brain vesicles (telencephalon, diencephalon, mesencephalon, metencephalon and myelencephalon) were clearly distinguishable. Both the anterior and posterior neuropores were closed. The optic vesicles were prominent in the forebrain region, and the otic pits were well defined. Two pharyngeal arches have appeared (Fig. 9a,c). The mandible component of the first pharyngeal arches and the forelimb buds have increased in size (Fig. 9a), but the hindlimb buds were not as well developed (Fig. 9b). The posterior intestinal portal was more narrow than then seen at earlier stages (compare Figs. 7a, 9a). Both the 9.5 dpc mouse embryo at stage 15 with 21-29 somites and stage 17HH chick embryo are representative of this stage.

As described for the Carnegie Stages XIII–XIV human embryos (Davis, 1927; Goor and Lillehei, 1975; Christoffels et al., 2000), the heart had lost its tubular features due to the expanding atrial and ventricular segments. At this age, some well-developed proepicardial protrusions were still present on the ventral wall of the sinus venosus (Fig. 9c); moreover, the epicardium was already covering the cardiac cavities (Fig. 9 d,f). Recently, Mannër (2009) designated this period as the "mature S-loop." In our case, the most notable observations were as follows: I. The positions of cardiac segments correlate with the formation of the cranial and cervical flexures as previously found Patten (1922) and Mannër et al. (1993) in chick. II. The laterally expanded atria had taken a dorso-superior position (Fig. 9c,d), with a wall comprised primarily of a nearly compact myocardial sleeve (Fig. 9d). III. The primordia of the trabeculated region of the right and left ventricles were situated inferior and adjacent to one another, with the interventricular groove in between (Fig. 9e). Both primordia displayed incipient myocardial trabeculations lined by endocardium (Fig. 9d,f), which had not yet grouped to form the interventricular septum. IV. The rudimentary "primitive cardiac septum" was formed by the septum primum with the foramen primum, the incipient dorsal or superior and ventral or inferior cushions of the AV canal and some small individual trabeculations. This embryonic

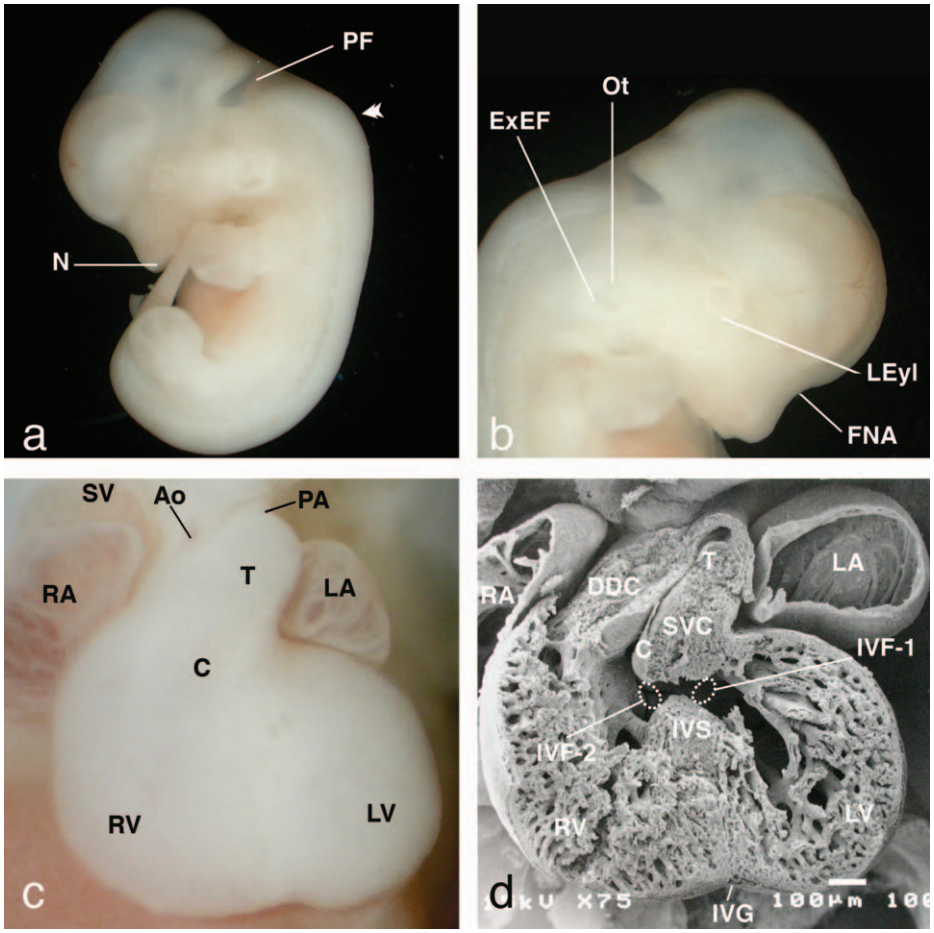

Fig. 14. Embryo at 14 days. **a, b**. Left and right views of the embryo. **a**. Notice the cervical flexure corresponding to the neck bending (Arrowhead). The hands and feet, with traces of digit condensation, and the growing nose (N) are also illustrated. **b**. Observe the ovoid otocysts (Ot), the external ear flap (ExEF), the fronto-nasal angle (FNA) and the lower eyelid (LEyl). **c, d**. Frontal view and scanning electron micrograph of the heart. d. Notice the interventricular groove (IVG) below the interventricular septum (IVS) with a reduced primary interventricular foramen (IVF-1) and the secondary interventricular foramen (IVF-2). Other abbreviations have been listed in previous figures.

structure was firstly described in the chick embryo heart at stage 17HH as a continuous septum whose anatomical features determine that the AV cushions partially divide what was previously the common primitive inlet into the right and left AV orifices (de la Cruz et al., 1983). Consequently, we speculate that at this age the primordium of the apical trabeculated region of each ventricle directly connects with its corresponding atrium by way of its own inlet. V. The primary interventricular foramen was bordered by some ventricular trabeculations and the superior and inferior AV cushions composed of scarce fibroblast-like cells immersed in an abundant amount of ECM (Fig. 9d). VI. As in the chick embryo heart at stage 16HH (García Peláez and Arteaga, 1993) the distal segment of the embryonic outflow tract ("truncus arteriosus") was morphologically distinct (Fig. 9c,e,f). It was facing a ventro-dorsal direction running over the superior wall of the primitive atria. VII. Inside both the proximal (conus) and distal (truncus arteriosus) segments of the embryonic outflow tract two incipient endocardial crests were observed containing very few fibroblast-like cells (Fig. 9f). VIII. The cephalic border of the "truncus arteriosus" was connected to the common aortic sac, which was not yet projected into the pericardial cavity (Fig. 9f).

It is worth mentioning that even though the distal segment of the embryonic outflow has classically been considered to be the primordium of the trunks of the main arteries, it has recently been described, in the chick embryo, that they also give rise to the insertion ring and arterial valves (Sánchez Gómez et al., 2005).

ED 12 embryos. Projection of the aortic sac into the pericardial cavity. The primary morphological difference at this developmental stage compared to earlier stages can be seen in the substantial changes that have taken place in the cephalic region. These changes are a result of the subdivision of the primitive forebrain vesicle into secondary brain vesicles that have markedly increased in volume (compare b and a in Fig. 8). A relatively shallow pontine flexure separates the metencephalon and myelencephalon (Fig. 10a,b). At this stage, the average length of the embryos was 6.2 mm. The optic vesicles have become less prominent. They are also more dorsally displaced and wedged between the

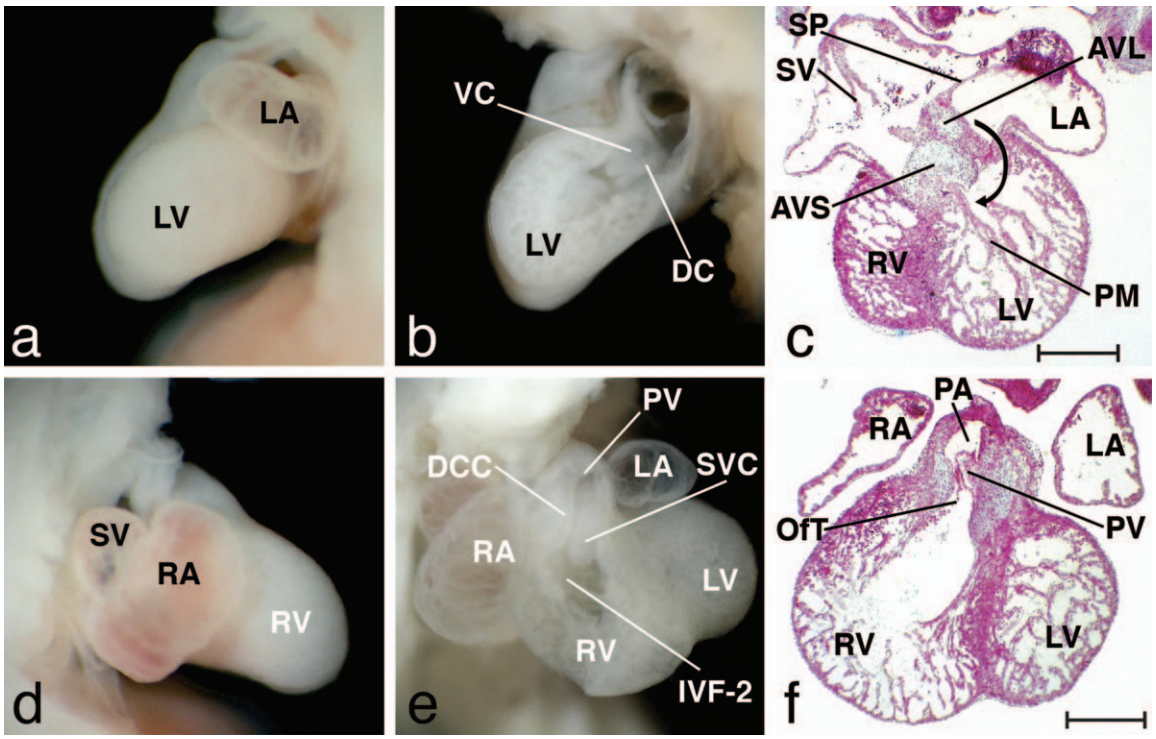

Fig. 15. Heart of embryo at 14 days. The left ventricle begins to acquire the outflow tract. **a, b**. External view and dissection of the left cavities of the heart. **b**. Observe the partially fused dorsal (DC) and ventral (VC) atrioventricular cushions. **c**. Frontal section of the heart. Notice the sinus venosus (SV), the developing atrioventricular septum (AVS) and the inlet of the left ventricle (arrow). Some lamellar atrioventricular leaflets (AVL) and incipient papillary muscles (PM) are also shown. **d, e, f**. Right views and frontal section of the heart. **e**. Notice the voluminous, nearly fused dextrodorsal (DDC) and sinistroventral (SVC) conus crests as well as the secondary interventricular foramen (IVF-2). **f**. Observe the almost mature pulmonary outflow tract (OfT), the developing pulmonary valves (PV) and the trunk of the pulmonary artery (PA). Abbreviations are as in previous figures. Scale bars = 0.35 mm.

telencephalon and the maxillary components of the first pharyngeal arches (Fig. 10a,b). The beginning of the nasal bud and the naso-lacrimal grooves can also be seen at this time (Fig. 10b). In some embryos, the third pharyngeal arches have begun to emerge. The otic pit has begun to separate from the overlying ectoderm (Fig. 10b), and nearly all of the embryos had 30 pairs of somites. The distal region of the tail has curled upon itself. All four limb buds were fin shaped, but the hindlimb buds were still less developed than the forelimbs (Fig. 10a). In general, the embryo morphology we observed was similar to that of a 10-10.25 dpc mouse embryo at stage 16 and a Carnegie Stage XV human embryo.

Interestingly, the external and internal features of the heart in ED 12 rat embryos correspond to those features in the stage 22HH and 24HH chick embryos. Similar to that described for stage 22HH chick embryos (de la Cruz, et al., 1983; de la Cruz, 1998a; de la Cruz et al., 1977; Mannër, 2000; Sánchez Gómez et al., 2005), we found that the primitive atria were more cephalodorsally positioned (Fig. 10c, 11) and that the sinus venosus occupied a dorso-inferior position relative to the primitive atria (Fig. 11d). The developing ventricles were in a caudo-ventral position (Fig. 10c, 11). The endocardial crests of the embryonic outflow tract were composed of spaced fibroblast-like cells and abundant ECM (Fig. 11e,f). The dextrodorsal and sinistroventral crests had partially divided the "conus" into two orifices (ventral or anterior and dorsal or posterior), both of which were connected to the developing right ventricle (Fig. 11e,f). Although the chick heart has been described as having three "truncal crests" (Qayyum et al., 2001), in rat we only observed a superior and an inferior "truncal crest" (Fig. 11e). Similar to the findings in the chick embryo, the "truncus" was connected to the aortic sac composed of mesenchyme internally covered by endothelium (Fig. 11f). As in the heart of the stage 24HH chick embryo (Contreras Ramos et al., 2008), the developing interventricular septum (IVS) was formed by a very small superior smooth region and a broad trabeculated caudal zone (Fig. 10d). Although the dorsal and ventral cushions of the AV canal had grown, they had not yet fused. In this case, the primary interventricular foramen was bordered by the developing interventricular septum and the dorsal and ventral cushions of the AV canal (Fig. 11b). Contrary to the finding in stage 22HH and 24HH chick embryos in which the common aortic sac had not yet projected into the pericardial cavity (Sánchez Gómez et al., 2005), in ED 12 rat embryos it was inside the pericardial cavity (Fig. 11c,f).

ED 13 embryos. End of the torsion and looping process of the heart tube and the division of the aortic sac into two ducts. The embryos had ~7.5 mm of length and 41 pairs of somites. At the same time,

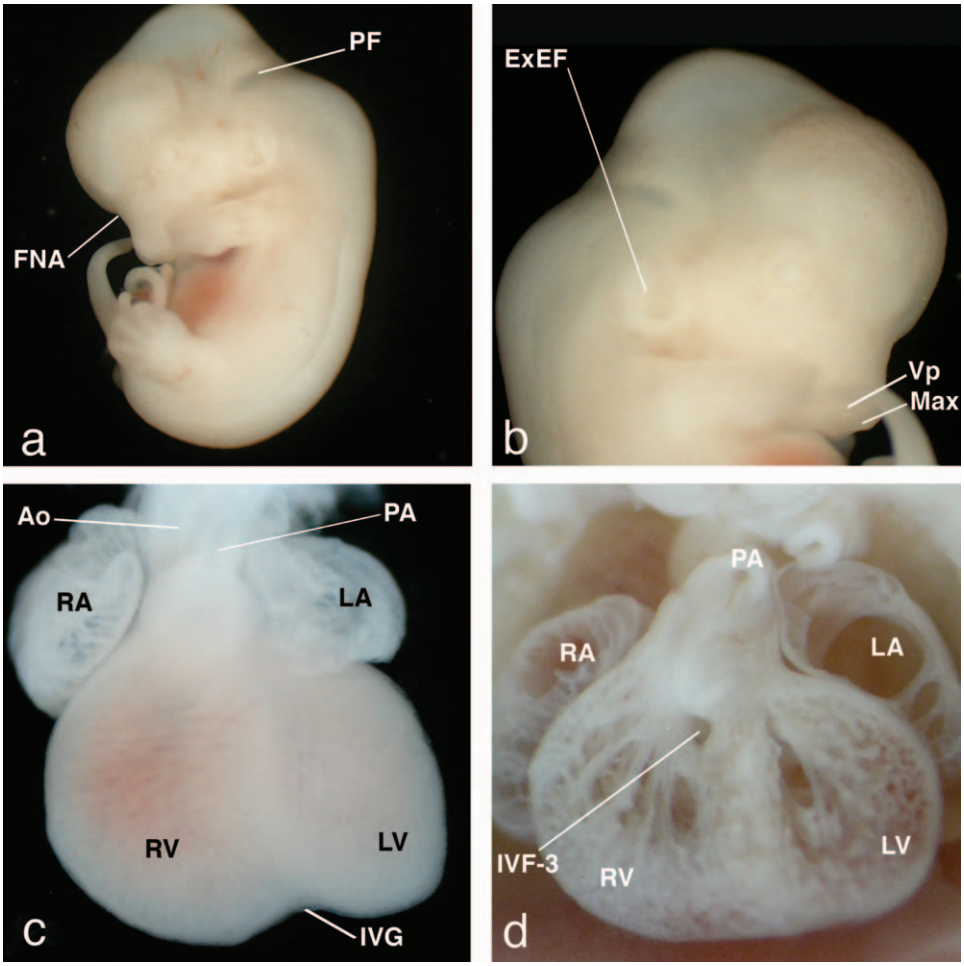

Fig. 16. Embryo at 15 days. **a, b**. Left and right views of the embryo. **a**. Notice the nearly completely closed pontine flexure (PF) and the fronto-nasal angle (FNA). **b**. Observe the emerging vibrissae papillae (Vp) on the maxilla (Max) and the incipient external ear flap (ExEF) **c, d**. Frontal view and dissection of the heart illustrate the interventricular groove (IVG) and a very small tertiary interventricular foramen (IVF-3) at the posterior boundary of the ventricular outflow tract. Other abbreviations have been listed in previous figures.

a marked increase in the overall volume of the cephalic region was observed (Figs. 8c, 12a,b). At this stage, the chondrification centers can first be identified. The pontine flexure and naso-lacrimal grooves were deeper than at earlier stages, but the metencephalon seems reduced (compare Figs. 10a,b with 12a,b). The lens vesicles were closed, the lateral and medial nasal prominences have come into contact, and the nasal pits have become deeper. The overlying tissue of the otic vesicles has thickened, and a deep groove has developed between the maxillary and mandible components of the first pharyngeal arches (Fig. 12b). The limb buds have become increasingly prominent. The paddle-shaped forelimb buds were at a slightly more advanced stage of limb differentiation than the fin-shaped hindlimb buds (Fig. 12a). The physiological umbilical hernia has become apparent for the first time and contains only a relatively small region of the midgut loop. These observations are in accordance with the previously described morphology of the 11 dpc mouse embryo at stage 17.

At this age, the developing atrial and ventricular cavities were situated in their appropriate location (Figs. 12c, 13). The foramen primum was facing the AV cushions (Fig. 13b), and the foramen secundum has started to develop in the superior border of the septum primum. The dorsal and ventral AV cushions were overlapping but had not yet fused (Fig. 13b), and the lateral (right and left) AV cushions have appeared (Fig. 13c). The caudal trabeculated zone of the developing interventricular septum has grown exponentially (Figs. 12d, 13f). Despite the smooth zone of the interventricular septum was already in contact with the dorsal and ventral AV cushions, an interventricular foramen in reference to the embryonic outflow was still present. Two voluminous endocardial crests partially was divided the proximal (conus) and distal (truncus) segments of the embryonic outflow tract into two orifices (Fig. 13e), but both components of the "conus" still seem to emerge from the developing right ventricle (Fig. 12d, 13e). Despite this finding, the posterior "conus" was advocated and connected to the left ventricle by way the interventricular foramen (Fig. 13f), while the anterior "conus" had transformed into the outlet for the right ventricle. The apparently reduced "truncus" had almost completely

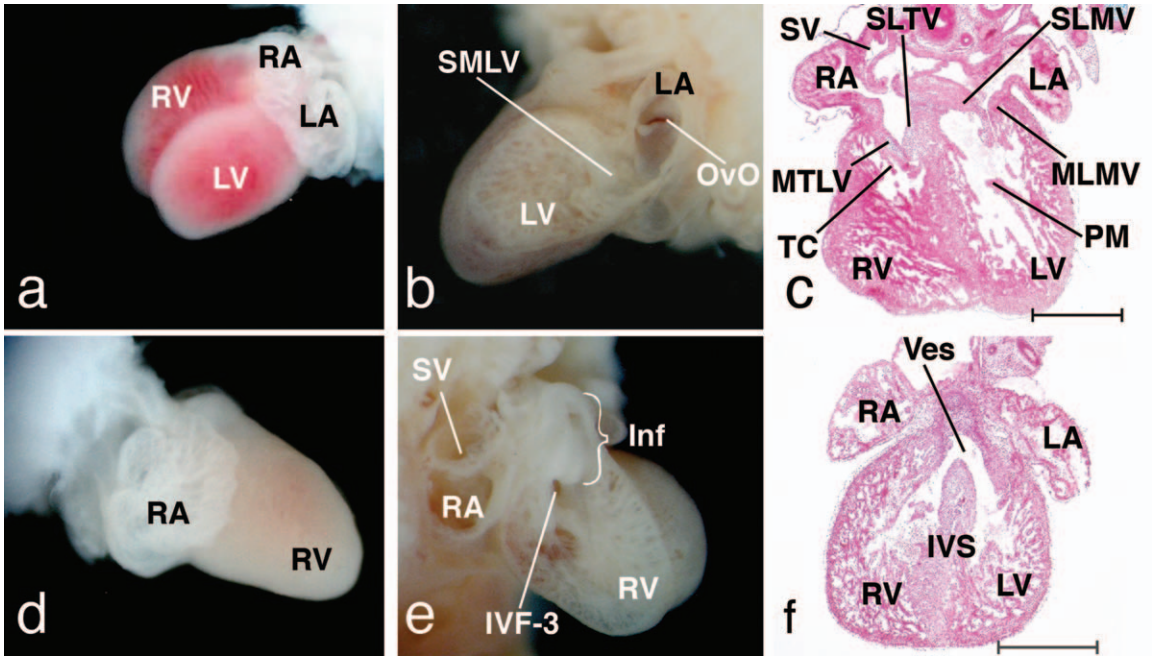

Fig. 17. Heart of embryo at 15 days. The left ventricle fully acquires its outflow tract. **a, b**. Tangential view of the heart and dissection of the left cardiac cavities. **b**. Observe the ovale orifice (OvO) and the immature septal leaflet of the mitral valve (SLMV). **c**. A frontal section of the heart illustrates the histological features of the immature atrioventricular valves, the incipient tendinous cords (TC) and papillary muscles (PM). **d, e, f**. Right views and frontal histological section of the heart. **e**. Observe the trabeculated nearly mature pulmonary outflow tract (Inf) emerging from the right ventricle (RV). **f**. Notice the left ventricle outflow tract (Ves) wedged in between the incomplete interventricular septum (IVS). MLMV = Mural leaflet of the Mitral valve; MLTV = Mural leaflet of the Tricuspid valve; SLMV = Septal leaflet of the mitral valve; SLTV = Septal leaflet of the tricuspid valve. Other abbreviations are as in previous figures. Scale bars = 0.5 mm.

transformed into the arterial valves internally (Fig. 13f), however, they still maintained a relatively ventro-dorsal direction, running over the interatrial sulcus (Fig. 13a,b) and connecting to the almost completely septated aortic sac (Fig. 13f). The external and internal cardiac features were nearly identical between the ED 13 rat embryo, stage 26HH chick embryo (de la Cruz et al., 1983; Anselmi and de la Cruz, 1998; Mannër, 2000; Sánchez Gómez et al., 2005; Contreras Ramos et al., 2008), and Carnegie Stage XVI human embryos (de Vries and Saunders, 1962; Netter and Van Mierop, 1969).

ED 14 embryos. The left ventricle has begun to acquire an outflow tract. The average length of the embryos at this stage was 9.5 mm. Because of the thickening of the exterior coat of the embryo, it was not possible to record somite number; however, chondrification was more general. The superior and inferior borders of the pontine flexure were closer than seen at the earlier stages (compare Figs. 12a, 14a). The lens vesicles were completely separated from the corneal epithelium, and the peripheral margin of the eyes has become well defined (Fig. 14b). The maxillary component of the first pharyngeal arch has become more prominent and is sharply defined. The olfactory pits were reduced to relatively narrow slits, and otocysts have become more ovoid than spherical in shape. The fronto-nasal angle, the external ear flap, and the lower eyelid have also begun to form at this stage (Fig. 14b). The neck was bent and the tail was narrow and elongated, with its caudal end often in close proximity to the developing nose (Fig. 14a). The limb buds were divided into proximal and distal parts, and the hand and foot plates showed traces of digit condensation (Fig. 14a). In general, the embryo morphology resembled that of an 11 dpc mouse embryos at St. 18.

The sinus venosus was located completely dorsal to the developing atria (Fig. 15c,d). The ventricular cavities were externally separated by a shallow interventricular groove, which corresponded internally to the developing IVS (Fig. 14c,d). The dorsal and ventral AV cushions have begun to fuse, and as a result, the atrioventricular septum has begun to appear (Fig. 15b,c). The primary interventricular foramen was reduced but the secondary interventricular foramen was observed between the interventricular septum, the right tubercles of the endocardial cushions and the sinistroventral conus ridge (Figs. 14d, 15e). The leaflets of the atrioventricular valves, tendineae cords, and papillary muscles have begun to develop (Fig. 15c). At this stage, the embryonic outflow tract was almost completely separated by two voluminous, though not yet fused, endocardial crests (Figs. 14c, 15e). The anterior "conus" connected to the developing right ventricle has taken on a trabeculated appearance (Fig. 15e,f). In contrast, the posterior "conus" was partially emerging out of the developing left ventricle. The distal segment of the embryonic outflow tract (truncus) had become a relatively short, right caudocephalic tubular structure (Fig. 14c,d), inside of which the arterial valves have begun to form (Fig. 15f). At this stage, the aortic sac was completely separated into the aortic and pulmonary artery

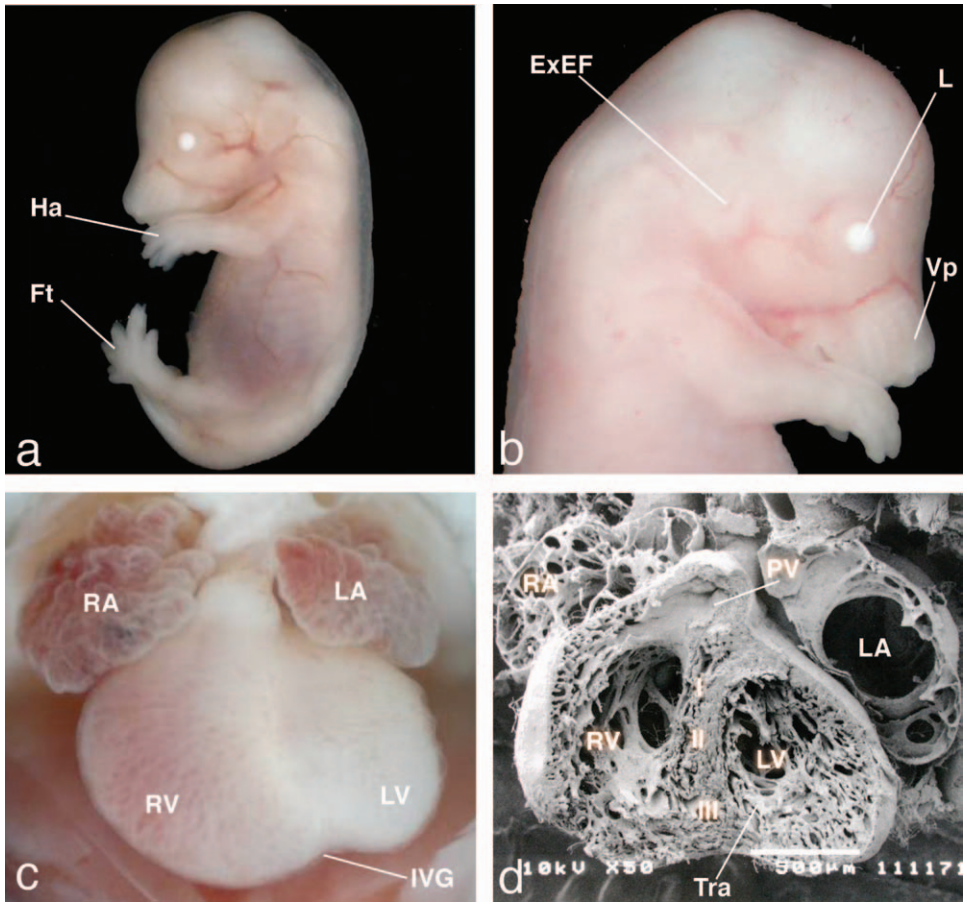

Fig. 18. Embryo at 16 days. **a, b**. Left and right views of the embryo show the nearly mature features of the body. **a**. Observe the separate digits in hand (Ha) and foot (Ft). **b**. Notice the nearly fully formed lens (L), the external ear flap (ExEF) and four rows of vibrissae papillae (Vp). **c, d**. Frontal view and dissection of the heart. **d**. Observe the basal (I) and medial (II) thirds of the interventricular septum facing the pulmonary valves (PV), while the apical third (III) displays a large amount of branched trabeculations (Tra). Abbreviations are as in previous figures.

trunks. A similar heart structure was described in the Carnegie Stage XVI-XVII human embryos (Goor and Lillehei, 1975) and in stage 28HH chick embryos (Sánchez Gómez et al., 2005; Contreras Ramos et al., 2008).

ED 15 embryos. The left ventricle fully acquires an outflow tract. The average length of the embryos at this age was 1.3 cm; the fronto-nasal angle was still present, while the superior and inferior boundaries of the pontine flexure were almost in contact (Fig. 16a). The first vibrissary papillae were observed on the maxillary prominences (Fig. 16b). The external ear flap and upper eyelid were more prominent than seen at previous stages (compare Fig. 14b, with Fig. 16b). The pharyngeal arches could no longer be distinguished superficially. The peripheral margins of both the hand and foot plates have taken a polygonal shape because of the presence of distinct digit interzones (Fig. 16a). The hair papillae have begun to appear. At this stage, ossification was first observed, which indicates the beginning of fetal period. Apart from these changes, the embryo morphology remained relatively unchanged. The findings are similar to those describing the morphology of 12-13 dpc mouse embryos (St. 20-21).

The heart had taken on more "mature" features (Figs. 16c,d and 17). The septum secundum and the ovale orifice had completely formed (Fig. 17b). The arterial valves, the leaflets of the AV valves, the tendinous cords and the papillary muscles have differentiated (Fig. 17c,f). Similar to that described by Goor and Lillehei (1975) in the Carnegie Stage XVIII human embryo, a very small tertiary interventricular foramen was observed at the posterior end of the ventricular outflow tract (Fig. 16d, 17f). As in the 29HH chick embryonic heart (Sánchez Gómez et al., 2005), the outflow tract of the right ventricle (infundibulum) had a trabeculated appearance and was connected to the ventro-lateral pulmonary artery trunk (Fig. 17e), while the outflow tract of the left ventricle (vestibule) was wedged between the IVS and connected to the aortic trunk (Fig. 17f).

As de la Cruz (1998b) and Sánchez Gómez et al, (2005) found in chick, we observed that initially both the anterior and posterior "conus" emerge from the immature right ventricle and that the outlet of this ventricle (infundibulum) begins to form as soon as the "conal"

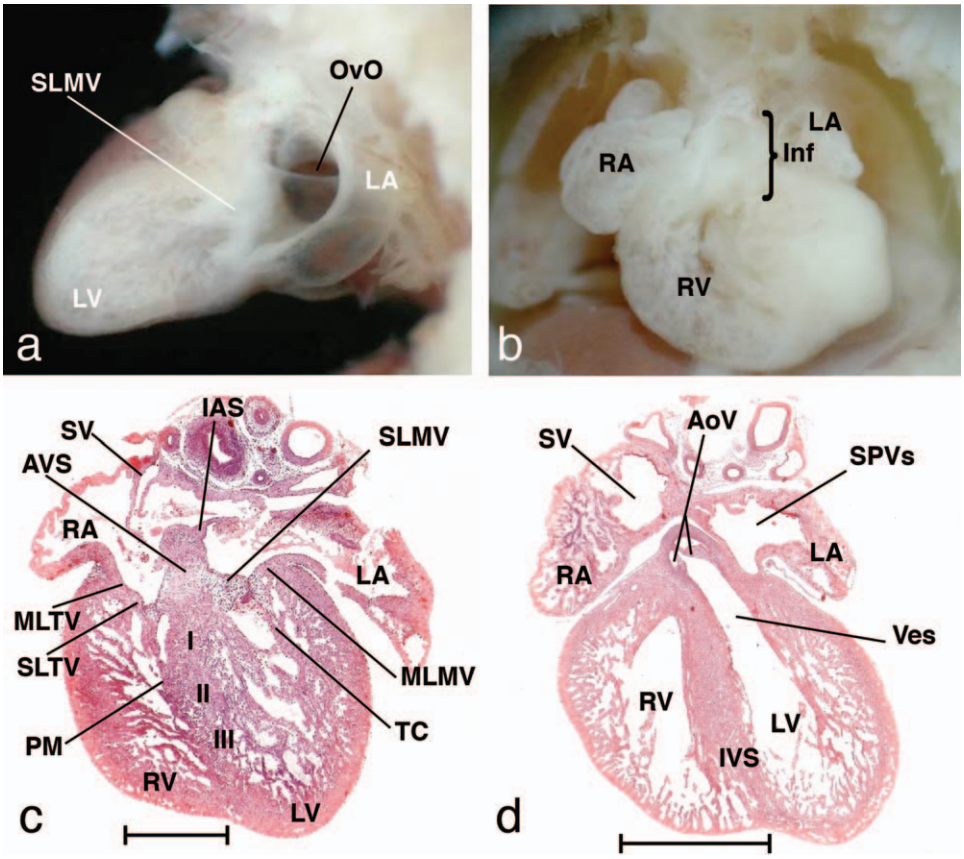

Fig. 19. Heart of embryo at 16 days. Mature heart. **a**. Dissection of the left cardiac cavities showing the oval orifice (OvO) and the developing septal leaflet of the mitral valve (SLMV). **b**. Dissection of the right ventricle (RV) and the infundibulum (Inf). **c, d**. Four-chambered sections of the heart. **c**. Observe the histological maturation of the right and the left atrioventricular valve apparatuses, as well as the three thirds (I, II, III) in the interventricular septum. **d**. Notice the aortic valve (AoV), the vestibulum (Ves), the entrance of the sinus venosus (SV) and that of the pulmonary veins (SPVs). Other abbreviations have been listed in previous figures. Scale bars = 0.5 mm.

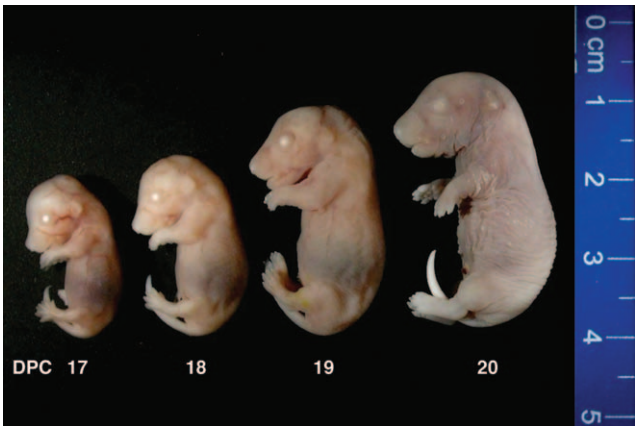

Fig. 20. Fetal age. External aspect of fetuses at 17–20 days postcoitum shows the substantial increase in crow to tail length.

ridges appear. In contrast, the development of the outlet of the LV (vestibule) takes place later, nearly at the end of cardiac septation. These results indicate that in both species (chick and rat) the incorporation of the posteromedial primitive outlet into the left ventricle is a very long and gradual process, which as proposed De la Cruz et al., in 2001 explains the wide spectrum of congenital pathologies of the ventricular outlets.

ED 16 embryos. Mature heart. The overall shape of the fetus had changed while the average length was 1.9 cm. Notably, the pronounced "hump" that is characteristically presents between the caudal hindbrain and upper cervical region of the 14-15 dpc embryos has almost completely disappeared (compare d with f in Fig. 8); the head has become quite erect, and the body was straight. Ossification centers were also more common. The face also appeared to have taken on more "adult" features, including a larger external ear flap, which was located more rostrally than observed at earlier stages (compare Figs. 16b, 18b). In addition, the external naris appeared to be almost fully developed, and the eyes appeared to have undergone further differentiation with respect to the lens. More than four rows of vibrissae papillae were present (Fig. 18b). The hair papillae were well developed, and division of the anterior paw into separate digits had commenced (Fig 18a). The distal part of the tail had become finer. General morphology of the ED

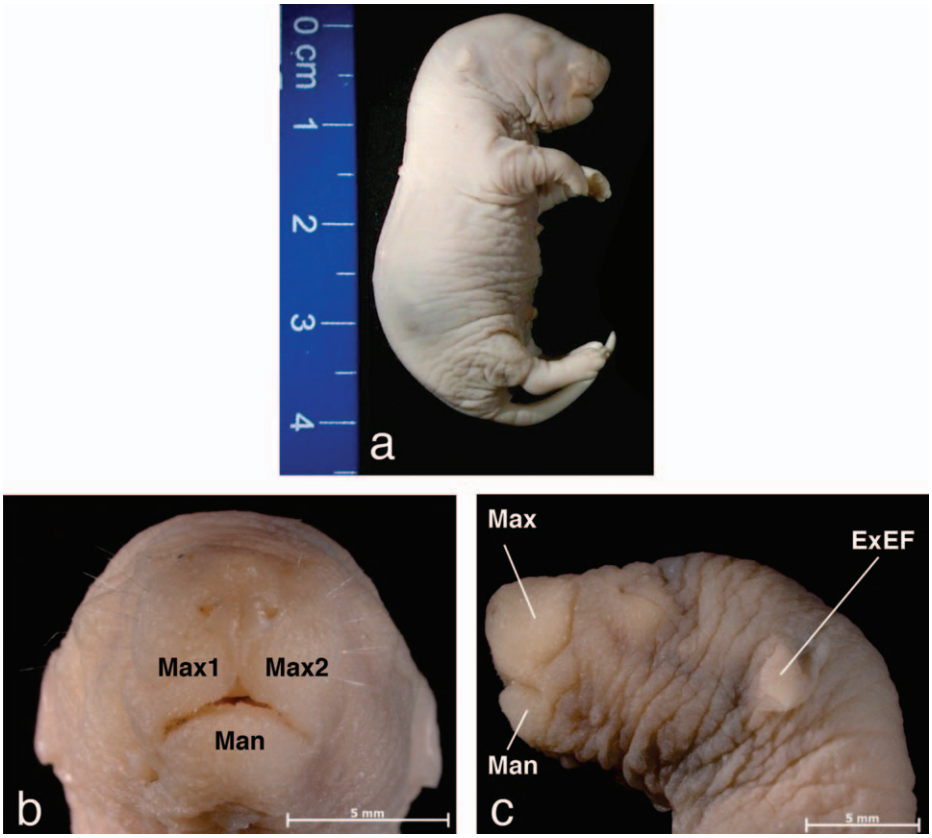

Fig. 21. Newborn rat. **a**. External features of a newborn rat. **b**. A frontal view of the face shows the almost completely fused maxillary prominences (Max1, Max2), the long whiskers and the permeable nasal pores. **c**. A sagittal view of the cephalic region of the newborn rat shows the long maxilla and the still closed eyes. Scale bars = 5 mm.

16 rat embryo was similar to that of the 14.5 dpc mouse (stage 22).

As previously described for the stage 30HH chick embryo (Contreras Ramos et al., 2008) and Carnegie Stage XIX human embryo (Goor and Lillehei, 1975), in the ED 16 embryo the heart was almost fully formed (Figs. 18c,d, 19). The interventricular foramen was completely closed and the interventricular septum displayed three zones (thirds). The apical third (in reference to the pointed end or apex of the heart) was composed of long branched trabeculations. The medial and basal thirds (facing the AV and arterial valves) were smooth and compact (Figs 18c, 19c,d). At this stage, histological analysis revealed that the right (tricuspid) and left (mitral) atrioventricular valve apparatuses as well as the arterial valves have begun to mature (Fig. 19c,d). Contrary to the findings described in humans (Goor and Lillehei, 1975), the sinus venosus and sinus of the pulmonary veins were not incorporated to the atria (Fig 19c,d).

Newborn

The more relevant developmental events in fetuses from 17 to 20 days and 21 days newborn (NB) include an increase in weight and crow to tail length. Aside from these changes, the fetus morphology remained almost the same, including the still closed eyes. (Figs. 20, 21). Approximately 2-cm long, 16-day-old fetus grew to a roughly 4-cm long newborn rat (Compare Fig. 18a with Figs. 20, 21a). In general, the external appearance of the NB rat was very similar to that of an ED 16 fetus (Compare Fig. 18A with Figs. 20, 21a). In these animals, the whiskers were longer and clearly visible; the maxillary prominences were fused, and the nasal pores opened. The sagittal view showed that the maxilla is longer than the mandible. The dark shadow on the left side of the body marked the location of the liver and spleen (Fig. 21c,d). Moreover, histological maturation of all the organs appears to be almost fully.

During this period, the heart and great vessels undergo very few morphological changes. We did not determine the topographical relationship between the pulmonary sinus, the sinus venosus, and the right atrium along heart development in rat as Männer and Merkel (2007) did in the chick embryo. Despite this, we found in the NB heart two right (inferior and superior) and one left (inferior) caval veins emerging from a pocket like structures at the posterior (dorsal) surface of the heart. In addition, three right and two left pulmonary veins were observed to emerge from a small pocket like structure connected to the left atrium (Fig. 22a).

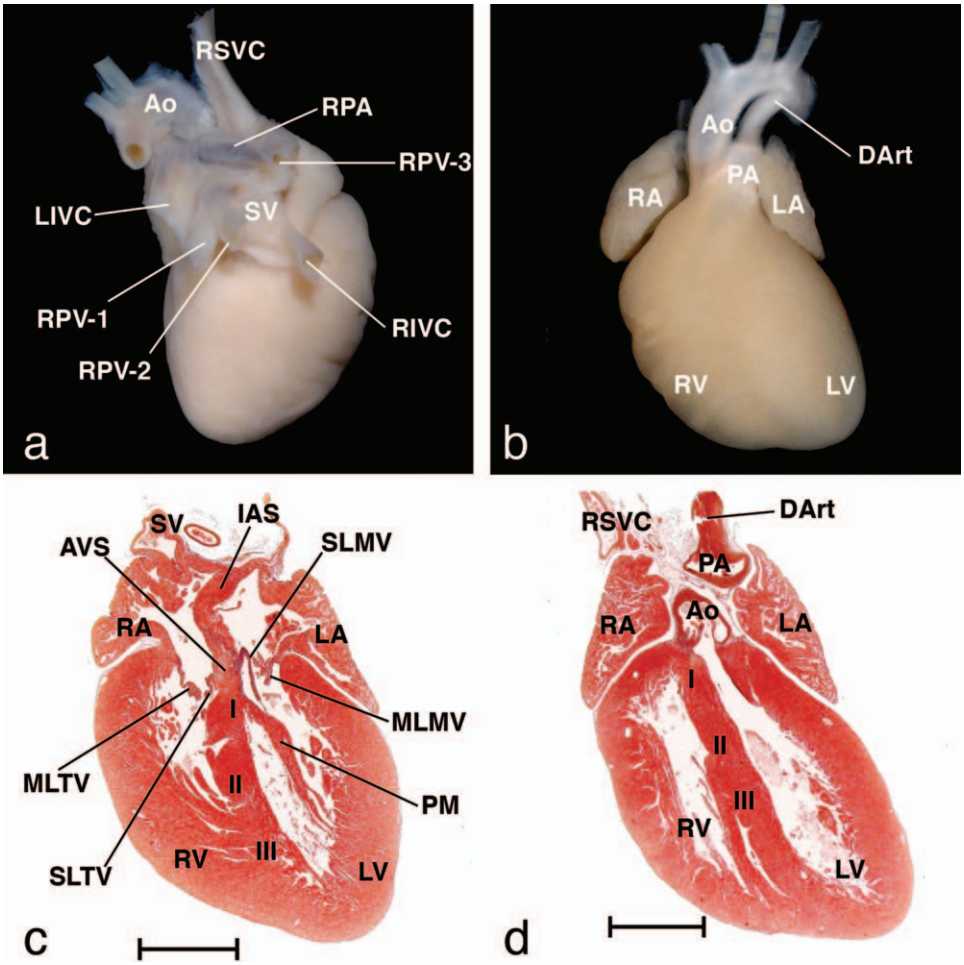

Fig. 22. Heart of the newborn rat. **a, b**. Dorsal and ventral views of the heart. **a**. Observe the pocket like sinus venosus partially integrated into the dorsal wall of the right atrium. **b.** Notice the ductus arteriosus vestige (DArt). **c, d**. Four-chambered sections depicting the histological features of the heart. AVS = atrioventricular septum; IAS = interatrial septum; LIVC = left inferior vena cava; MLMV = mural leaflet of the mitral valve; MLTV = mural leaflet of the tricuspid valve; RIVC = right inferior vena cava; RSVC = right superior vena cava; RPA = right pulmonary artery; RPV = Right pulmonary vein; SLMV = septal leaflet of the mitral valve; SLTV = septal leaflet of the tricuspid valve. Other abbreviations have been listed in previous figures. Scale bars = 1 mm.

These results indicate that in rat the sinusal region is only partially integrated into the dorsal wall of the right atrium (Fig. 22a). As in the NB mouse (Thieller 1989), we found in the rat that the ovale orifice was permeable, but the ductus arteriosus was impermeable and vestigial (Fig 22b,d). At this stage, the cardiac septa as well as the atrioventricular and arterial valve apparatuses were histologically more mature than at earlier stages (compare Figs. 19, 22c,d).

CONCLUSIONS

The morphological changes and fate of the embryonic components of the heart described in this study for the rat were primarily based on prior *in vivo* labeling studies carried out in the chick (Table 1). Descriptions of rat embryo, fetus, and postnatal morphologies correlated with the findings for both mouse and human development (Table 2). In general, nearly all the features (external and internal) of embryonic chick and rat heart were similar. We did observe, however, at least four main differences which may be important to researchers interested in studying the teratogenic, molecular and genetic aspects of cardiac development: (1) The anterior heart field in rat begins to transform into the embryonic outflow earlier and faster than in the chick. (2) The embryonic rat heart at ED 12 shares external and internal features with the heart of chick embryos at stages 22HH and 24HH. (3) In rat, the lateral AV cushions first appeared before fusion of the dorsal and ventral AV cushions. In contrast, these events occur nearly simultaneously in the chick. (4) Integration of the right systemic and left pulmonary sinus into the dorsal wall of the definitive atria in higher vertebrates has diverse ranges. In the tetracameral heart of humans, they are completely incorporated into the atria, but are partially or completely separated from the atria in rat and chick, respectively.

TABLE 1. Chronology of embryonic development and cardiac morphogenesis in the rat

Embryonic day	Pairs of somites	Main embryonic features	Main cardiac features
9		Tree-layered cup. Fully elongated primitive streak.	Two bilateral cardiogenic areas.
9 + 10 h	5	U-shaped embryo. Neural groove and incipient inverted U-shaped intestinal portal present.	Horseshoe-shaped cardiac crescent ventrally positioned beneath the foregut.
9 + 15 h	7–8	U-shaped embryo. Neural folds closed in somitic region. Identifiable otic rhombomere and optic placode	Bilaterally symmetric primitive cardiac tube. Two primordia: Apical trabeculated region of the right (RV) and left (LV) ventricles. Anterior heart field begins to specify.
	9	Partially formed neural tube. Well-defined optic pit foveae. Conspicuous maxillary components of the first branchial arch.	C-shaped loop. Five primordia: 1, 2. Apical trabeculated region of the RV and LV; 3. Primitive inlet (AV region); 4, 4′. Right and left primitive atria; 5. Incomplete proximal segment of the embryonic inlet (conus).
10	16–18	Straight embryonic body. Closed rostral and opened caudal neuropores. Three well-delimited primary brain vesicles present. Incipient otic placode. Conspicuous second branchial arch. Rudimentary anterior limb buds.	Immature S-loop. Cephalo-dorsal primitive atria connected by the common inlet (AV region) with the ventro-caudal primordium of the apical trabeculated region of the LV. Proximal segment of the embryonic outlet emerges from the future apical trabeculated region of the RV.
11	24	Smoothly delineated secondary brain vesicles. Closed anterior and posterior neuropores. Prominent primary optic vesicles. Well-defined otic pit. Three pharyngeal arches. Distinguished anterior and posterior limb buds.	Mature S-loop. Dorso-cephalic laterally expanded atria. Rudimentary septum primum and superior and inferior AV cushions. Inferior ventricular region. Two Incipient endocardial crests are located inside the embryonic outflow tract. Aortic sac not yet projected into the pericardial cavity. Cardiac cavities covered by epicardium.
12	30	Well-delimited secondary brain vesicles. Shallow pontine flexure. Rudimentary naso-lacrimal grooves, nasal bud and the fourth branchial arch present. Fin-shaped limb buds.	Dorsal and ventral AV cushions not yet fused. Conspicuous interventricular septum. Both orifices of the proximal segment of the embryonic outflow tract emerge from the RV. Distal segment connected to the common aortic sac projected into the pericardial cavity.
13	41	Voluminous cephalic region. Deep pontine flexure and nasolacrimal grooves. Closed lens vesicle. Lateral and medial nasal processes are in contact. Deep groove present between the maxilla and mandible. Paddle-shaped forelimb buds. Fin-shaped hindlimb buds. First appearance of chondrification	Atria and ventricles in appropriate locations. Incipient ostium secundum and overlapping dorsal and ventral AV cushions. Rudimentary right and left AV cushions. Persistent primary interventricular foramen. Both orifices of the proximal segment of the embryonic outflow tract emerge from the RV. The distal segment connected with the partially septated aortic sac.
14	Recording not possible	Reduced pontine flexure. Prominent maxillary component of the first branchial arch. Ovoid otocysts. Rudimentary earflap and lower eyelid present. Limb buds divided into proximal and distal segments. Traces of digit condensation. More general chondrification.	Fused dorsal and ventral AV cushions. Interventricular foramen closed at the ventricular inlets. Embryonic outflow tract separated by two voluminous but unfused endocardial crests. Outflow tract of the RV well developed. The LV begins to acquire its outflow tract. Distal segment of the embryonic outflow tract connected with the septated aortic sac.
15		Pontina flexure nearly closed. Pronounced external earflap and upper eyelid present. Superficially undistinguishable branchial arches. Digit interzones apparent in the hand and foot plates. Incipient first vibrissary and hair papillae. First manifestation of ossification and beginning of fetal period.	Completely formed septum secundum and ovale orifice. Developing AV leaflets, tendinous cords, papillary muscles and arterial valves. Small interventricular orifice at the posterior end of ventricular outflow tracts. Trabeculated pulmonary outflow tract present. The LV fully acquires its outflow tract.
16		Poorly visible "hump" between hindbrain and cervical region. Almost fully differentiated external auricle, naris and eye lenses. Hair papillae well developed.	Mature heart. Interventricular foramen completely closed. Almost compact interventricular septum.
21		Newborn pup. Eyes still closed whiskers longer and clearly visible; the maxillary processes quite fused, maxilla longer than mandible. Opened nasal pores.	Sinus venosus and pulmonary veins not totally integrated to the atria. Three right and two left pulmonary veins. Permeable Ovale orifice, impermeable Ductus arteriosus. Partially mature cardiac septa valves and tendinea cords.

TABLE 2. Milestones of early heart development in various species

Cardiogenic events	Rat ED	Mouse ED (Theiler's Stage)	Chick HH	Human Carnegie Stage (Streeter Horizons)
Cardiogenic areas	9	7.0 (St 10)	4	VI–VII (Second week)
Cardiac crescent	9 + 10h 5 ps	7.5 (St 11) 4–5 ps	7 first ps	IX (first ps, 20 days)
Straight heart tube	9 + 15h 7–9 ps	8.0 (St 12) 6–8 ps	9 + 8 ps	X (4 ps, 22 days)
C-shaped loop		8.0–8.5 (St 13) 8–12 ps	12 14–16 ps	X (7 ps, 23 days)
Immature S-shaped loop	10 16–18 ps	8.5–9 (St 14) 13–22 ps	14 22 ps	XI (13–28 ps, 25 ± 1 days)
Mature S-shaped loop and beginning of cardiac septation	11 24 ps	9.5 (St. 15) 21–29 ps	17 29–32 ps	XII-XIIIV (around 30 ps, 28–29 days)
Projection of the aortic sac into the pericardial cavity	12 30 ps	10–10.25 (St. 16) 30–34 ps	22–24	XV (30 ± 1 days)
Ending of the torsion and looping process; aortic sac divided into two conducts	13 around 41 ps	10.5 (St. 17) approximately 35–39 ps	26	XVI (31–34 days)
Left ventricle begins to acquire its outflow tract	14	11–11.5 (St. 18–19) 40–45 ps	28	XVI-XVII (36 ± 1 days)
Left ventricle acquires its outflow tract	15	12–13 (St. 20–21)	29	XVIII (37 ± 1 day)
Mature heart; completely closed interventricular foramen	16 Beginning of fetal period	14.5 (St. 22) Beginning of fetal period	30–32	XIX (38 ± 1 day)
Newborn heart	21	19	21	38 weeks

Rat data are based on our current study, while mouse information is from Theiler, (1989); Kaufman, (1999), and Parmacek and Leiden, (1999). Chick details are from Rawles, (1943); Stalsberg and DeHaan, (1965); de la Cruz et al., (1977, 1989, 1998). Human data are based on Davis, (1927); Streeter, (1942); de Vries and Sounders, (1962); Netter and Van Mierop, (1969); Goor and Lillehei, (1975); O'Rahilly and Muller, (1987). ED = embryonic day; HH = Hamburger and Hamilton stages (1951); ps = pairs of somite.

ACKNOWLEDGEMENTS

The authors are grateful to Ramón M Coral-Vázquez PhD. Sección de Posgrado, Escuela Superior de Medicina, IPN, México, DF & Subdirección de Enseñanza e Investigación, CMN "20 de Noviembre" ISSSTE, México, DF, generously provided RNA probes against mouse Nkx2.5 mRNAs, Jesús Chimal PhD, Instituto de Investigaciones Biomédicas UNAM, for ISH technical assistance and comments. Mario Jáuregui Castro, Oswaldo Aguirre Luna and Victor Manuel Hernandez Patiño for their technical assistance.

LITERATURE CITED

Anderson RH, Webb S, Brown NA, Lamers W, Moorman A. 2003. Development of the heart: (3) formation of the ventricular outflow tracts, arterial valves, and intrapericardial arterial trunks. Heart 89:1110–1118

Anselmi G, de la Cruz MV. 1998. Embryological development of the atria. Septation and viscero-atrial situs. In: de la Cruz MV, Markwald R, editors. Living morphogenesis of the heart. Boston, Basel, Berlin: Birkhäuser. p 169–186.

Aitman TJ, Critser JK, Cuppen E, Dominiczak A, Fernandez-Suarez XM, Flint J, Gauguier D, Geurts AM, Gould M, Harris PC, Holmdahl R, Hubner N, Izsvák Z, Jacob HJ, Kuramoto T, Kwitek AE, Marrone A, Mashimo T, Moreno C, Mullins J, Mullins L, Olsson T, Pravenec M, Riley L, Saar K, Serikawa T, Shull JD, Szpirer C, Twigger SN, Voigt B, Worley K. 2008. Progress and prospects in rat genetics: a community view. Nature Genetics 40: 516–522.

Castro-Quezada A, Nadal-Ginard B, de la Cruz MV. 1972. Experimental study of the formation of the bulboventricular loop in the chick. J Embryol Exp Morphol 27:623–637.

Christie GA. 1963. Developmental stages in somite and post-somite rat embryos, based on external appearance and including some features of the macroscopic development of the oral cavity. J Morph 114:263–286.

Christoffels VM, Habets PEMH, Franco D, Campione M, de Jong F, Lamers WH, Bao ZZ, Palmer S, Biben Ch, Harvey RP, Moorman AFM. 2000. Chamber formation and morphogenesis in the developing mammalian heart. Dev Biol 223:266–278.

Contreras Ramos A, Sánchez Gómez C, Garcia Romero H, Cimarosti L. 2008. Normal development of the muscular region of the interventricular septum. I. The significance of the ventricular trabeculations. Anat Histol Embryol 37:344–351.

Daston G, Faustman E, Ginsberg G, Fenner-Crisp P, Olin S, Sonawane B. 2004. A framework for assessing risks to children from exposure to environmental agents. Environ Health Perspect 112: 238–256.

Davis CL. 1927. Development of the human heart from its first appearance to the stage found in embryos of twenty paired somites. Carnegie Contrib Embryol 19:245–284.

De la Cruz MV. 1998a. Torsion and looping of the cardiac tube and primitive cardiac segments. Anatomical manifestations. In: de la Cruz MV, Markwald R, editors. Living morphogenesis of the heart. Boston, Basel, Berlin: Birkhäuser. p157–168.

De la Cruz MV. 1998b. Embryological development of the outlet of each ventricle. In: de la Cruz MV, Markwald R, editors. Living morphogenesis of the heart. Boston, Basel, Berlin: Birkhäuser. p 99–120

De la Cruz MV, Castillo MM, Villavicencio L, Valencia A, Moreno-Rodríguez R. 1997. Primitive interventricular septum, its primordium, and its contribution in the definitive interventricular septum: in vivo labeling study in the chick embryo heart. Anat Rec 247:512–520.

De la Cruz MV, Giménez-Ribotta M, Saravalli O, Cayré R. 1983. The contribution of the inferior endocardial cushion of the atrioventricular canal to cardiac septation and to the development of

the atrioventricular valves: study in the chick embryo. Am J Anat 166:63–72.

De la Cruz MV, Markwald R, editors. 1998. Living morphogenesis of the heart. Boston, Basel, Berlin: Birkhäuser.

De la Cruz MV, Markwald R, Krug E, Rumenoff L, Sánchez Gómez C, Sadowinski S, Galicia TJ, Gómez F, Salazar GM, Villavicencio GL, Reyes A, Moreno Rodríguez RA. 2001. Living morphogenesis of the ventricles and their regional congenital pathology. Cardiol Young 11:588–600.

De la Cruz MV, Sánchez GC, Arteaga M, Argüello C. 1977. Experimental study of the development of the truncus and the conus in the chick embryo. J Anat 123:661–686.

De la Cruz MV, Sánchez Gómez C. 1998. Straight tube heart. Primitve cardiac cavities vs. primitive cardiac segments. In: de la Cruz MV, Markwald R, editors. Living morphogenesis of the heart. Boston, Basel, Berlin: Birkhäuser. p85–98.

De la Cruz MV, Sánchez Gómez C, Robledo Tovi JL. 1987. Experimental study of the development of the ventricular inlets in the chick embryo. Embryologische Hefte 1:25–37.

De la Cruz MV, Sánchez Gómez C, Palomino MA. 1989. The primitive cardiac regions in the straight tube heart (stage 9-) and their anatomical expression in the mature heart: an experimental study in the chick embryo. J Anat 165:121–131.

De la Cruz MV, Sánchez Gómez C, Cayré R. 1991. The developmental components of the ventricles: their significance in congenital cardiac malformations. Cardiol Young 1:123–128.

De Vries PA, Saunders JB. 1962. Development of the ventricles and spiral outflow tract in the human heart. A contribution to development of the human heart from age group IX to age XV. Contrib Embryol 256:89–114.

García Peláez I, Arteaga M. 1993. Experimental study of the development of the truncus arteriosus of the chick embryo heart. Anat Rec 237:378–384.

Geurts AM, Cost GJ, Freyvert Y, Zeitler B, Miller JC, Choi VM, Jenkins SS, Wood A, Cui X, Meng X, Vincent A, Lam S, Michalkiewicz M, Schilling R, Foeckler J, Kalloway S, Weiler H, Ménoret S, Anegon I, Davis GD, Zhang L, Rebar EJ, Gregory PD, Urnov FD, Jacob HJ, Buelow R. 2009. Knockout Rats via embryo microinjection of zinc-finger nucleases. Science 325:433.

Goor DA, Lillehei CW. 1975. Congenital malformations of the heart. Embryology, anatomy and operative considerations. New York: Grune and Stratton.

Hamburger B, Hamilton HL. 1951. A series of normal stages in the development of the chick embryo. J Morphol 88:49–92.

Heikinheimo M, Scandrett JM, Wilson DB. 1994. Localization of transcription factor GATA 4 to regions of the mouse embryo involved in cardiac development. Dev Biol 164:361–373.

Kaufman MH. 1999. The Atlas of mouse development. London: Academic Press, Harcourt Brace & Co.

Linash KK, Lash JW. 1987. Precardiac cell migration: Fibronectin localization at mesoderm-endoderm interface during directional movement. Dev Biol 114:87–101.

Lints TJ, Parson LM, Hartley L, Lyons I, Harvey RP. 1993. *Nkx2.5*, a novel murine homeobox gene expressed in early heart progenitor cells and their myogenic descendant. Development (Cambridge, UK) 119:419–431.

Mannër J. 2000. Cardiac looping in the chick embryo: a morphological review with special reference to terminological and biomechanical aspects of the looping process. Anat Rec 259: 248–262.

Mannër J. 2009. The anatomy of cardiac looping: a step towards the understanding of the morphogenesis of several forms of congenital cardiac malformations. Clin Anat 22:21–35.

Mannër J, Merkel N. 2007. Early morphogenesis of the sinuatrial region of the chick heart: a contribution to the understanding of the pathogenesis of direct pulmonary venous connections to the right atrium and atrial septal defects in hearts with right isomerism of the atrial appendages Anat Rec 290:168–180.

Mannër J, Seidl W, Steding G. 1993. Correlation between the embryonic head flexures and cardiac development. An experimental study in chick embryos. Anat Embryol (Berl) 188:269–285.

Marinho MA, Sala RA, Lopes MF, de Moraes Grisi AB, Novaes, Jr, de Souza SLS, Taba M, Jr. 2007. Teratogenic effects of the interaction acetylsalicylic acid (ASA) and ethanol: morphologic and morphometric evaluation of the lingual epithelium in rat fetuses. Anat Histol Embryol 36:14–18.

Mashimo T, Yanagihara K, Tokuda S, Voigt B, Takizawa A, Nakajima R, Kato M, Hirabayashi M, Kuramoto T, Serikawa T. 2008. An ENU-induced mutant archive for gene targeting in rats. Nature Genetics 40:514–515.

Monti J, Fischer J, Paskas S, Heinig M, Schulz H, Gösele C, Heuser A, Fischer R, Schmidt C, Schirdewan A, Gross V, Hummel O, Maatz H, Patone G, Saar K, Vingron M, Weldon SM, Lindpaintner K, Hammock BD, Rohde K, Dietz R, Cook SA, Schunck W-H, Luft FC, Hubner N. 2008. Soluble epoxide hydrolase is a susceptibility factor for heart failure in a rat model of human disease. Nature Genetics 40:529–537.

Moorman A, Webb S, Nigel A, Brown NA, Lamers W, Anderson RH. 2003. Development of the heart: (1) formation of the cardiac chambers and arterial trunks. Heart 89:806–814.

Netter FH, Van Mierop LHS. 1969: Embryology. In: Netter FH, editor. CIBA collection of medical illustrations. Ardsley, New Jersey: CIBA Pharmaceutical Co. 5:119–125.

O'Rahilly R, Muller F. 1987. Developmental stages in human embryos. Washington: Carnegie Contrib Embryol 637.

Parameswaran M, Tam PPL. 1995. Regionalization of cell fate and morphogenetic movement of the mesoderm during mouse gastrulation. Dev Genet 17:16–28.

Parmacek MS, Leiden JM. 1999. GATA transcription factors and cardiac development. In: Harvey RP and Rosenthal N, editors. Heart development. Boston: Academic Press. p 291–306.

Patten BM. 1922. The formation of the cardiac loop in the chick. Am J Anat 30:373–397.

Petretto E, Sarwar R, Grieve I, Lu H, Kumaran KM, Muckett PhJ, Mangion J, Schroen B, Benson M, Punjabi PP, Prasad SK, Pennell DJ, Kiesewetter Ch, Tasheva ES, Corpuz LM, Webb MD, Conrad GW, Kurtz TW, Kren V, Fischer J, Hubner N, Pinto YM, Pravenec M, Aitman TJ, Cook SA. 2008. Integrated genomic approaches implicate osteoglycin (Ogn) in the regulation of left ventricular mass. Nature Genetics 40:546–552.

Qayyum RS, Webb S, Anderson RH, Verbeek FJ, Brown NA. 2001. Septation and valvar formation in the outflow tract of the embryonic chick heart. Anat Rec 264:273–283.

Rawles ME. 1943. The heart-forming areas of the early chick blastoderm. Physiol Zool 16:22–44.

Redkar A, Montgomery M and Litvin J. 2001. Fate map of early avian cardiac progenitor cells. Development 128, 2269–2279.

Rice D, Barone G. 2000. Critical periods of vulnerability for the developing nervous system: evidence from humans and animal models. Environ Health Persperct 108:511–533.

Sánchez Gómez C, Pliego PL, Contreras Ramos A, Munguía Rosas MA, Salazar GM, García Romero HL, González Jiménez MA. 2005. Histological study of the proximal and distal segments of the embryonic outflow tract and great arteries. Anat Rec 283A: 202–211.

Simán CM, Gittenberger-DeGroot A, Wisse AB, Ericksson UJ. 2000. Malformations in offsprings of diabetic rats: morphometric analysis of neural crest- derived organs and effects of maternal vitamin E treatment. Teratology 61:355–367.

Stalsberg H, deHaan RL. 1969. The precardiac areas and formation of the tubular heart in the chick embryo. Dev Biol 19: 128–159.

Streeter GL. Developmental horizon in human embryos. 1942. Description of age group XI, 13 to 20 somites and age group XII, 21 to 29 somites. Carnegie Contrib Embryol 30: 211–230.

Tam PPL, Parameswaran M, Kinder SJ, Weinberger RP. 1997. The allocation of epiblast cells to the embryonic heart and other mesodermal lineages: the role of ingression and tissue movement during gastrulation. Development (Cambridge, UK) 124: 1631–1642.

Tam PL, Schoenwolf GC. 1999. Cardiac fate maps: lineage, allocation, morphogenetic movement, and cell commitment. In: Harvey RP, Rosenthal N, editors. Heart development. Boston: Academic Press. p 3–18.

Theiler K. 1989. The house mouse: atlas of embryonic development. New York, Berlin, Heidelberg: Springer Verlag New York Inc.

Twigger SN, Pruitt KD, Fernández-Suárez XM, Karolchik D, Worley KC, Maglott DR, Brown G, Weinstock G, Gibbs RA, Kent J, Birney E, Jacob HJ. 2008. What everybody should know about the rat genome and its online resources. Nature Genetics 40: 523–527.

Ya J, Van den Hoff MJ, de Boer PA, Tesink-Taekema S, Franco D, Moorman AF, Lamers WH. 1998. Normal development of the outflow tract in the rat. Circ Res 82:464–472.

Zaffran S, Kelly RG, Meilhac SM, Buckingham ME, Brown NA. 2004. Right ventricular myocardium derives from the anterior heart field. Circ Res 95:261–268.